

Western  Graduate&PostdoctoralStudies

Western University  
**Scholarship@Western**

---

Electronic Thesis and Dissertation Repository

---

8-20-2015 12:00 AM

# Supplementation With Hydrogen Sulfide Helps Mitigate The Effects Of Ischemia Reperfusion Injury In A Model Of Donation After Cardiac Death Renal Transplantation

Jaskirandeep Kaur Grewal  
*The University of Western Ontario*

Supervisor  
Dr. Alp Sener  
*The University of Western Ontario*

Graduate Program in Microbiology and Immunology  
A thesis submitted in partial fulfillment of the requirements for the degree in Master of Science  
© Jaskirandeep Kaur Grewal 2015

Follow this and additional works at: <https://ir.lib.uwo.ca/etd>



Part of the [Urology Commons](#)

---

## Recommended Citation

Grewal, Jaskirandeep Kaur, "Supplementation With Hydrogen Sulfide Helps Mitigate The Effects Of Ischemia Reperfusion Injury In A Model Of Donation After Cardiac Death Renal Transplantation" (2015). *Electronic Thesis and Dissertation Repository*. 3053.  
<https://ir.lib.uwo.ca/etd/3053>

This Dissertation/Thesis is brought to you for free and open access by Scholarship@Western. It has been accepted for inclusion in Electronic Thesis and Dissertation Repository by an authorized administrator of Scholarship@Western. For more information, please contact [wlsadmin@uwo.ca](mailto:wlsadmin@uwo.ca).

SUPPLEMENTATION WITH HYDROGEN SULFIDE HELPS MITIGATE THE  
EFFECTS OF ISCHEMIA REPERFUSION INJURY IN A MODEL OF DONATION  
AFTER CARDIAC DEATH RENAL TRANSPLANTATION

(Thesis format: Monograph)

by

Jaskirandeep Kaur, Grewal

Graduate Program in Microbiology and Immunology

A thesis submitted in partial fulfillment  
of the requirements for the degree of  
Master of Science

The School of Graduate and Postdoctoral Studies  
The University of Western Ontario  
London, Ontario, Canada

© Jaskirandeep K. Grewal 2015

## Abstract

Donation after cardiac death (DCD) grafts experience prolonged ischemia reperfusion injury (IRI) leading to higher rates of delayed graft function and failure. Recent studies have reported protective effects of hydrogen sulfide (H<sub>2</sub>S) against IRI. Our study aims at improving DCD renal graft outcomes by H<sub>2</sub>S supplementation in an *in-vivo* murine model of renal transplantation (RTx) and study the underlying mechanism in an *in-vitro* model using porcine kidney proximal-tubular-epithelial cells (LLC-PK1). H<sub>2</sub>S provided survival benefit, improved renal graft function and decreased renal injury in recipient rats. In our *in-vitro* model of LLC-PK1 cells, H<sub>2</sub>S demonstrated an important role mediated by mitochondria in the pathophysiological effects of IRI by reducing depolarization of the mitochondrial membrane and the amount of reactive oxygen species. In the long run, these findings would help bridge the gap between organ demand and supply by reducing the extent of renal IRI and delayed graft function in DCD donors.

## Keywords

Ischemia reperfusion injury, donation after cardiac death, kidney transplantation, rats, hypoxia, porcine kidney cells, hydrogen sulfide, gasotransmitters, reactive oxygen species, mitochondria, apoptosis, necrosis.

## Co-Authorship Statement

The following people and institutions contributed to the work undertaken as part of this thesis:

Jaskirandeep Kaur Grewal, University of Western Ontario

Dr. Jifu Jiang, Matthew Mailing Centre for Translational Transplant Studies, London Health Sciences Centre

Dr. Aaron Haig, University Hospital, London Health Sciences Centre

### **Roles and contribution to thesis:**

Jaskirandeep Kaur Grewal is the primary candidate for this thesis.

Dr. Jifu Jiang is the microsurgeon that performed all the surgeries related to the *in-vivo* model of this project.

Dr. Aaron Haig is the pathologist who scored the H&E stained histological sections of the tissues collected from the rats.

## Acknowledgments

I would like to thank my supervisor, Dr. Alp Sener, for his support and guidance throughout my project. In addition, I want to thank my advisory committee members Dr. Zhuxu Zhang and Dr. Sung Kim, for helping me with the development of my project. A special thanks to Dr. Manujendra Saha and Ian Lobb, for training me on various lab techniques. Lastly, I would like to thank my family and friends for all the encouragement and emotional support.

# Table of Contents

Abstract .....	ii
Co-Authorship Statement.....	iii
Acknowledgments.....	iv
Table of Contents .....	v
List of Tables .....	ix
List of Figures .....	x
List of Appendices .....	xii
List of Abbreviations, Symbols and Nomenclature .....	xiii
Chapter 1 .....	1
1 Introduction .....	1
1.1 Kidney Disease .....	1
1.2 Treatment Options for ESRD.....	2
1.2.1 Dialysis: definition and types.....	2
1.2.2 Advantages and disadvantages associated with dialysis.....	3
1.2.3 Renal transplant .....	3
1.2.4 Types of organ donors .....	4
1.2.5 Pros and cons of renal transplant .....	5
1.2.6 Effectiveness of renal transplant over dialysis.....	6
1.3 Ischemia/Reperfusion Injury.....	7
1.3.1 IRI effects at cellular level.....	7
1.4 Gasotransmitter family.....	10
1.4.1 Nitric oxide and carbon monoxide.....	11
1.4.2 Hydrogen Sulfide .....	13
1.5 Hydrogen sulfide and IRI.....	15

1.5.1	Inflammation and H <sub>2</sub> S.....	15
1.5.2	Antioxidant effect .....	16
1.5.3	Protecting mitochondrial integrity and anti-apoptotic role.....	16
1.5.4	H <sub>2</sub> S donor molecules.....	17
1.6	Rationale, Hypotheses and Aims .....	21
1.6.1	Rationale .....	21
1.6.2	Hypotheses .....	21
1.6.3	Aims.....	21
Chapter 2	.....	23
2	Materials and Methods.....	23
2.1	Murine Model of Donation after Cardiac Death (DCD) Renal Transplantation ..	23
2.1.1	Animal description and care .....	23
2.1.2	Preliminary experiments and final experimental design.....	23
2.1.3	Surgical procedure .....	24
2.1.4	Post-operative monitoring.....	25
2.1.5	Assessment of graft renal function and injury .....	25
2.1.6	Renal histopathology .....	26
2.1.7	RNA isolation, cDNA synthesis and real time PCR.....	27
2.1.8	Data analysis .....	28
2.2	DCD model in LLC-PK1 cells.....	31
2.2.1	LLC-PK1 cell line.....	31
2.2.2	Synthetic hydrogen sulfide donor used.....	31
2.2.3	Experimental design.....	31
2.2.4	Viability analysis .....	32
2.2.5	Quantification of reactive oxygen species .....	33
2.2.6	Detection of mitochondrial membrane depolarization .....	34

2.2.7	Measuring mRNA expression of apoptosis related proteins.....	34
2.2.8	Data analysis .....	35
Chapter 3	.....	37
3	Results .....	37
3.1	Murine Model of Donation after Cardiac Death.....	37
3.1.1	Increased survival in treatment group rats .....	37
3.1.2	Serum analysis indicates a trend of improved graft function in treatment group .....	38
3.1.3	Urine analysis demonstrates reduced injury in treatment group.....	39
3.1.4	ATN scores depict higher histological injury in untreated rats .....	39
3.1.5	Comparable amount of apoptosis observed in the untreated and treatment group renal transplant recipients .....	40
3.1.6	Trends in mRNA expression of pro-apoptotic, anti-apoptotic and inflammatory markers in the collected tissue .....	40
3.2	<i>In-vitro</i> DCD Model .....	50
3.2.1	GY4137 improved cell viability and decreased necrosis and late apoptosis in LLC-PK1 cells experiencing IRI .....	50
3.2.2	GY4137 supplementation indicated a trend in reduction of cells with detectable ROS.....	51
3.2.3	Trend depicting decline in depolarization of the mitochondrial membrane in cells treated with GY4137 .....	51
3.2.4	Up-regulation of anti-apoptotic proteins and down-regulation of injury related proteins in treated cells following hypoxia .....	52
Chapter 4	.....	60
4	Discussion .....	60
Chapter 5	.....	66
5	Future Directions.....	66
Chapter 6	.....	67
6	Conclusion and Significance.....	67



Bibliography .....	68
Appendices.....	83
Curriculum Vitae .....	85

## List of Tables

Table 1. Criteria for classification of a gasotransmitter.....	10
Table 2. Primer sequences (rat) used in qRT-PCR reactions.....	30
Table 3. Primer sequences for qRT-PCR in LLC-PK1 cell samples.....	36

## List of Figures

Figure 1: Mitochondria associated apoptotic pathway. ....	9
Figure 2: Endogenous production of NO and CO in cells. ....	12
Figure 3: Enzymatic pathway for endogenous production of hydrogen sulfide.....	14
Figure 4: Chemical equation for synthesis of GYY4137.....	20
Figure 5: Finalized experimental design for <i>in-vivo</i> murine model of DCD renal transplantation.....	29
Figure 6: D-Cysteine and H <sub>2</sub> S supplementation improved survival of renal transplant recipients.. ....	41
Figure 7: D-Cysteine and H <sub>2</sub> S supplementation indicates a trend of accelerated recovery in renal graft function following ischemic injury to the renal grafts .....	42
Figure 8: (A) Serum urea levels depict similar trends as serum creatinine and (B) serum osmolality remains consistent across different experimental groups over the time course of experiment.....	43
Figure 9: Urine protein to creatinine ratio indicating inferior kidney function in the untreated group rats in comparison to the treatment group rats .....	45
Figure 10: Decreased urine osmolality in the renal transplant recipients in comparison to the sham-operated rats .....	46
Figure 11: H <sub>2</sub> S supplementation reduces tissue injury following ischemia reperfusion injury .....	47
Figure 12: Number of apoptotic cells in kidney tissue collected from untreated group and treatment group of rats on post operative day 30.....	48
Figure 13: Differences in the mRNA expression of various apoptosis related genes. ....	49

Figure 14: Different combinations of warm and cold hypoxic times and resulting impact on cell viability. ....	53
Figure 15: Flow analysis scatter plots obtained from Annexin-V and 7-AAD staining.....	54
Figure 16: Increased percentage of viable cells upon supplementation with GYY4137.....	55
Figure 17: Trend depicting decrease in percentages of necrotic and late apoptotic cells after supplementation with H <sub>2</sub> S donor.. ....	56
Figure 18: Trend indicating reduction in percentage of cells with reactive oxygen species upon H <sub>2</sub> S supplementation.....	57
Figure 19: Trend depicting decreased percentage of cells with depolarized mitochondrial membrane in treated sample. ....	58
Figure 20: Up-regulation of anti-apoptotic proteins while down regulation of injury markers observed with H <sub>2</sub> S supplementation. ....	59

## List of Appendices

Appendix A: Preliminary data showing graft recovery following renal transplantation with grafts that had experienced IRI .....	83
Appendix B: Ethics approval form for <i>in-vivo</i> experiments .....	84

## List of Abbreviations, Symbols and Nomenclature

7-AAD	7 Aminoactinomycin D
ATN	Acute Tubular Necrosis
ATP	Adenosine Tri-phosphate
CAT	Cysteine Amino Transferase
cDNA	Complimentary Deoxyribonucleic Acid
CKD	Chronic Kidney Disease
CBS	Cystathionine Beta Synthase
CSE	Cystathionine Gamma Synthase
CVD	Cardiovascular Disease
DAO	D-amino Acid Oxidase
DBD	Donation after Brain Death
DCD	Donation after Cardiac Death
DEPC	Diethylpyrocarbonate
DHR 123	Dihydrorhodamine 123
DMEM	Dulbecco's Modified Eagle's Medium
DMSO	Dimethyl Sulfoxide
DNA	Deoxyribonucleic Acid
eNOS	Endothelium Nitric Oxide Synthase
ESRD	End Stage Renal Disease

FBS	Fetal Bovine Serum
GFR	Glomerular Filtration Rate
GY4137	Morpholin-4-ium 4-methoxyphenyl (morpholino) Phosphinodithioate
H&E	Hematoxylin and Eosin
HO	Heme Oxygenase
iNOS	Inducible Nitric Oxide Synthase
I.P.	Intraperitoneal
IRI	Ischemia Reperfusion Injury
LLC PK1	Porcine Proximal Tubular Epithelial Kidney Cells
MAPK	Mitogen Activated Protein Kinase
MMPT	Mitochondrial Membrane Permeability Transition
MOMP	Mitochondrial Outer Membrane Permeabilization
mRNA	Messenger Ribonucleic Acid
3-MST	3-Mercaptopyruvate Synthase
NADP	Nicotinamide Adenine Dinucleotide Phosphate
NKF	National Kidney Foundation
NMDA	N-methyl D-aspartate
NOS	Nitric Oxide Synthase
nNOS	Neuronal Nitric Oxide Synthase
PARIS	Protein and RNA isolation Kit

PBS	Phosphate Buffered Saline
PLP	Pyridoxal 5'-phosphate
QOL	Quality of Life
qRT-PCR	Quantitative Real Time Polymerase Chain Reaction
RNA	Ribonucleic Acid
ROS	Reactive Oxygen Species
RRT	Renal Replacement Therapy
TNF- $\alpha$	Tumor Necrosis Factor Alpha
TUNEL	Deoxynucleotidyl-Transferase-Mediated dUTP Nick End Labeling
UW	University of Wisconsin Solution



# Chapter 1

## 1 Introduction

### 1.1 Kidney Disease

Kidneys are one of the vital organs in our body responsible for maintaining the normal physiological conditions. On average, a person's kidneys weigh around 115grams and are responsible for processing about 180 liters of blood to remove waste and toxic products such as urea and ammonium along with excess water.<sup>1</sup> Being the major excretory organs besides the gastrointestinal tract, they also play a role in metabolic and biosynthetic functions such as the regulation of renin that regulates blood volume and pressure<sup>1</sup>, and red blood cell formation via erythropoietin synthesis.<sup>1,2</sup>

In some individuals, the kidneys stop working optimally and this leads to chronic kidney disease (CKD). CKD, as defined by the National Kidney Foundation (NKF), is either kidney damage or decreased kidney function [as measured by decreased Glomerular Filtration Rate (GFR) of less than 60mL/min/1.73m<sup>2</sup>] for three or more months.<sup>3</sup> The loss of kidney function is gradual and can remain undetected for a long time. Currently, there are 26 million American adults that have CKD and several others are at an increased risk.<sup>2</sup> Some factors that are known to increase a person's vulnerability to the development of CKD are high blood pressure/chronic hypertension, diabetes and old age.<sup>2,3</sup> About 50% of kidney failure cases are linked to diabetes while 30% are associated with hypertension.<sup>4</sup> Other conditions such as polycystic kidney disease, lupus, glomerulonephritis and malformations during embryonic development may also affect the kidneys leading to a greater risk of CKD.<sup>3</sup>

NKF has identified and classified CKD into five different stages based on the severity of kidney function loss measured by decreased GFR. Progression of CKD from its mild-asymptomatic stages to the late stages happens gradually. The final stage of CKD is called the End Stage Renal Disease (ESRD) and is often described as the kidney failure with the GFR being less than 15mL per minute per 1.73m<sup>2</sup>.<sup>1</sup> Upon progression into this

stage, the patient either needs to receive regular dialysis treatments or undergo renal transplantation.

## 1.2 Treatment Options for ESRD

The prevalence rate for ESRD in 2012 was reported to be 1182 per million in Canada and has been increasing for the past few years.<sup>5</sup> The ESRD patients experience a lot of physical conditions including but not limited to fatigue, anorexia, pain, sleep problems, anxiety and depression.<sup>6</sup> In addition, the risk of developing cardiovascular diseases in patients suffering from ESRD is almost 100 times of what is expected in the average population.<sup>7</sup> The treatment options available to the ESRD patients are summed under the term renal replacement therapy (RRT) and include dialysis and renal transplant.<sup>8</sup> In 2012, about 58% of the ESRD patients were being treated with dialysis while 42% were living with a functional kidney transplant in Canada.<sup>5</sup>

### 1.2.1 Dialysis: definition and types

Dialysis, at a biochemical level, is defined as the separation of substances in solution by means of their unequal diffusion across a semipermeable membrane.<sup>9</sup> In medical terms, it generally refers to the removal of wastes or toxins from the blood and restoring the electrolyte and fluid balance by the use of differential diffusion rates of different substances through a semipermeable membrane.<sup>10</sup>

There are two types of dialysis – hemodialysis and peritoneal dialysis.<sup>11</sup> Hemodialysis came into practice in 1960's<sup>10</sup> and is the most commonly used method of dialysis. It requires access to the patient's circulatory system.<sup>9,10</sup> The blood is pumped into the dialyzer for filtration from the artery. Following the removal of excess fluids and waste products, it is pumped back into the vein. The semi-permeable membranes installed in the dialyzer help carry out the process of diffusion. On the other hand, peritoneal dialysis involves the use of peritoneum as the semi-conservative membrane that enables the exchange of electrolytes, fluids and waste products.<sup>12</sup> The major difference between these two types of dialysis is that hemodialysis needs assistance of medical personnel and is generally carried out in designated sections of hospitals while the peritoneal dialysis can

be carried out at home without visiting any medical facility.<sup>10,13</sup> However, both types of dialysis are life saving and help in improving a patient's quality of life.<sup>14,15</sup>

### 1.2.2 Advantages and disadvantages associated with dialysis

The major advantage for dialysis treatments is zero wait times associated with the initiation of the procedure. When an individual is diagnosed with CKD and needs external assistance in the filtration of blood, immediate help is available at medical facilities upon physician's recommendation. However, some disadvantages include experiencing a feeling of being sick following the dialysis treatment due to the drainage of energy, incidents of hypo/hyper-tension, muscle cramping, restless leg syndrome, anemia and nausea / vomiting.<sup>16,17</sup> In addition, the hemodialysis treatment involves spending several hours three times a week at the hospital, thereby compromising the quality of life of these patients.<sup>12,14</sup> The frequency and time of the treatments impose a lot of limitations on a patient's life such as travel, ability to work and time commitment.

### 1.2.3 Renal transplant

Renal transplant is defined as the medical procedure involving the placement of the donor kidney into the patient suffering from ESRD.<sup>18</sup> It is the treatment of choice for most ESRD patients and generally happens after a prolonged time of dialysis treatments due to the nature of the timeline involved in receiving a transplant. The process begins when the physician prognosis ESRD in the patient and continues until a suitable donor kidney is available. However, the whole process of finding a donor kidney is time consuming and can take up to 3-7 years from the time of placement on the waitlist to receiving a kidney transplant.<sup>19,20</sup>

As a result of the long wait times, many ESRD patients who do not have a living donor available, die waiting for a donor organ. According to the United States Renal Data System, 4270 patients died in the year 2014 while waiting for a renal transplant and another 3617 patients became too sick to receive the transplant.<sup>18,21</sup> Yet, the wait list continues to grow with each passing year.<sup>21</sup>

### 1.2.4 Types of organ donors

There are two categories of organ donors that are used for renal transplantation – living donors and deceased/cadaveric donors.<sup>8</sup> The ideal group for organ donation is the living donors. A living donor (for renal transplantation) is an individual who donates one kidney to someone in need of a transplant (ESRD patient) as the donor can survive on a single healthy kidney. In most cases, the living donor is somehow related to the recipient and this helps to reduce the wait time for finding a biologically compatible donor kidney [based on blood group (ABO) and human leukocyte antigen (HLA) compatibility]. On the other hand, the organs from the deceased donors are procured after declaration of brain or cardiac death. Generally speaking, the growing wait times for receiving a deceased donor's kidney are due to the limited number of organ donors and increased number of patients along with the significant number of kidneys that are deemed unsuitable for transplantation (discarded organs).<sup>8</sup>

In 2012, a total of 17,305 kidney transplants were performed in United States which included 5617 kidneys from living donors and 11,535 kidneys from the deceased donor pool.<sup>21</sup> This shows that the deceased donors contribute a larger proportion of the total kidney transplants performed than do the living donors. Unfortunately, kidneys donated by the deceased donors have a four percent higher chances of graft failure (measured by factors like the patient's return to dialysis, repeat transplantation or death) in comparison to that from living donors.<sup>21</sup>

Further, in order to meet the organ shortage, the regulations for selecting deceased donor kidneys for transplantation have become less stringent. Until the year 2005, the only acceptable deceased organ donors for renal transplantation were the ones that belonged to a younger age group (19 - 44 years old) who had died from brain injuries, often referred to as the brain dead donors or donation after brain death (DBD).<sup>22,23</sup> In these cases, minimal injury was experienced by the donated kidneys because the blood supply to the kidney was intact. However, the number of organs from the brain dead donors and living donors were not enough to meet the organ demand in USA.

The other potential opportunity to meet the organ shortage was the use of donation after cardiac death (DCD) organs. DCD is widely accepted as an important source of organ procurement in other developed countries like United Kingdom and Australia.<sup>22</sup> However, the use of DCD organs was limited in Canada until the year 2005. The new ethical guidelines and policies that came into effect the same year permitted the use of DCD donors in Canada.<sup>24,25</sup> The rate of DCD transplants has increased eight fold over the last two decades.<sup>26</sup> The DCD donors are of two types – controlled and uncontrolled. The uncontrolled DCD donors are found to be dead upon arrival and have either not been resuscitated or resuscitated unsuccessfully.<sup>26</sup> The controlled DCD organ donors are typically the patients in intensive care units receiving life-sustaining treatments that have suffered a non-recoverable brain injury. However, they fail to fulfill the criteria for the donation after brain death. In these cases, permission is requested from the patient's family prior to the planned withdrawal of life support leading to a controlled DCD.<sup>27</sup>

After the withdrawal of life-support, a period of time passes until death can be pronounced by cardiac arrest. This time period is highly variable during which time the organs are vulnerable to ischemic. Following cardiac arrest, death cannot be pronounced until five minutes after. Thereafter, the donor is taken to the operation room for organ procurement. Upon procurement, the organs are perfused with the cold storage solution until the time of transplantation in the recipient.<sup>28</sup>

In the controlled DCD, the procured organs experience longer periods of warm ischemic stress during the period of time between discontinuation of life support and pronouncement of death. This is further exacerbated by the long periods of cold storage (cold ischemia) time leading to complications in the graft functioning upon transplantation.<sup>24,28,29</sup> As a result, the risk of delayed graft function and primary non function rate are significantly increased in DCD renal transplants (compared to DBD organs) thereby necessitating the need for dialysis during the first week following transplantation.<sup>27,30,31</sup>

### 1.2.5 Pros and cons of renal transplant

The major determinant of patient outcomes after transplantation is the long wait time experienced by the patients on the waitlist before receiving the transplant. On average, a

person encounters 3.6 years of wait time before receiving a transplant.<sup>21</sup> Due to the long wait times, the patients spend more years on dialysis which increases the risks of cardiovascular disease associated mortality in these patients.<sup>32</sup> In addition, patients experience increased risk of infection and cancer associated with the immunosuppressive drugs taken for the rest of their lives in order to prevent graft rejection.<sup>32-34</sup>

### 1.2.6 Effectiveness of renal transplant over dialysis

Renal transplantation offers ESRD patients an improved quality of life (QOL), increased life expectancy or survival advantage, decreasing the insults to cardiovascular system thereby lowering risk of cardiovascular diseases (CVD), decreased mortality and lower economic burden/costs.<sup>35-38</sup>

Many studies have reported a higher quality of life in patients that undergo renal transplantation to their counterparts that remained on the wait list with regular dialysis treatments.<sup>32,35,36</sup> The major factors that contribute to the improved quality of life in renal transplant recipients include physical function/ability, greater independence, engagement in social and recreational activities, and increased ability to work.<sup>25</sup> In addition to improved QOL, a 41% - 68% decrease in mortality has been reported in renal transplant recipients in comparison to those that tend to remain on the wait list.<sup>39,40</sup>

Over years, maintenance dialysis increases the risk of CVD associated mortality while the patients that are able to maintain the graft function following renal transplantation show continuous low CVD associated death rates, implying a long term reduction in the disease progression.<sup>41</sup> In addition to the various medical benefits, there is a 3.5 fold more expensive to remain on dialysis versus a renal transplant. Surprisingly, renal transplantation and maintenance cost much less (~\$250,000 less over a period of 5 years) than dialysis in the long term.<sup>37,42</sup>

All the above-mentioned factors make renal transplantation a better option for patients affected with ESRD.

## 1.3 Ischemia/Reperfusion Injury

Ischemia/reperfusion injury (IRI) is a pathological condition. As the name suggests, IRI is made up of two parts – ischemia and reperfusion. Ischemic injury happens when the blood supply to the organ is cut off leading to limited delivery of nutrients and oxygen.<sup>43</sup> Reperfusion follows ischemia with the subsequent restoration of the blood supply to the specific organ. Paradoxically, the restoration of blood supply to the organ enhances the cellular inflammatory responses that lead to IRI.<sup>44</sup> It is known to be inevitable in the donated organs thereby impacting the functionality of the grafts after transplantation.

### 1.3.1 IRI effects at cellular level

There are multiple ways in which IRI can cause damage to a cell and these damages ultimately result in cell death through apoptosis, necrosis or autophagy.<sup>43</sup> Apoptosis is caused by the action of intracellular signaling pathways that involve cellular caspases (caspase 3 and caspase 9). These caspases cleave the cytoskeletal proteins leading to the breakdown of the subcellular components.<sup>45,46</sup> The main characteristics observed during apoptosis are the shrinkage of the nucleus and cell, chromatin condensation and nuclear fragmentation.<sup>47</sup> Necrosis, on the other hand, is the cell death caused by swelling and eventual bursting. It happens due to the loss in integrity of cell membrane causing influx of the extracellular ions and fluid.<sup>47</sup> Autophagy is different from apoptosis and necrosis. It occurs on a daily basis and is defined as a pre-programmed cell death by means of which the cells are able to recycle the unnecessary or damaged organelles and macromolecular components.<sup>48,49</sup> However, under conditions of hypoxic stress and nutrient deprivation, our body uses this mechanism to provide the required substrates to the cells for metabolism.<sup>47</sup>

During IRI, the hypoxic conditions limit the availability of oxygen molecules. The cells need oxygen as the final acceptor of electrons in the electron transport chain in mitochondria. Due to the lack of oxygen, the powerhouses of the cell (mitochondria) produce reduced amount of energy in the form of adenosine triphosphate (ATP) molecules and fulfill the needs of the cell.<sup>50,51</sup> As a result, a number of ATP dependent ion channels in the cell membrane fail to function properly and it gradually leads to the

imbalance of cytoplasmic ions such as calcium ( $\text{Ca}^{+2}$ ), sodium ( $\text{Na}^{+}$ ) and hydrogen ( $\text{H}^{+}$ ).<sup>50</sup> This can lead to calcium overload that activates calcium dependent enzymes resulting in cell death or apoptosis. The hypoxic conditions also trigger the production of reactive oxygen species (ROS) in the mitochondria. These are free radicals and reactive molecules generated by molecular oxygen in the mitochondrial electron transport chain and include superoxides, hydroxyl anions and hydrogen peroxides. In addition, the hypoxic stress can cause the depolarization of mitochondrial membrane leading to a transition in the mitochondrial membrane permeability (MMPT).<sup>50,52</sup> Due to the decreased membrane potential, high molecular weight molecules are now able to freely pass through the mitochondrial membrane into the cytoplasm through the special channels and cause cellular damage.<sup>53</sup>

There are a number of proteins induced by I/R that play a major role in apoptosis and act in the mitochondria. The most well studied among these is the B-cell lymphoma (Bcl) protein family, which contains both pro-apoptotic (Bax, Bid) and anti-apoptotic members (Bcl-2, Mcl-1). It has been shown that the apoptotic process is initiated by caspase-8 that truncates the cytosolic protein Bid into tBid (Figure 1). The truncated tBid binds to the external mitochondrial membrane leading to the activation of Bax and Bak.<sup>54</sup> Upon activation, these proteins tend to oligomerize in the mitochondrial outer membrane triggering the channels in the mitochondrial membrane that cause leakage of cytochrome c into the cytoplasm.<sup>55</sup> When cytochrome c reaches the cytoplasm, it mediates formation of the apoptosome auto activating caspase 9. Active caspase 9 feeds the conversion of pro-caspase 3 into active caspase 3 which triggers eventual apoptosis.<sup>56,57</sup>

Endogenously produced gaseous messenger molecules (gasotransmitters – discussed in the upcoming section) have been shown to be helpful in mitigating some effects of IRI however, their mechanism of action has not been elicited yet and is of great interest to the scientists.



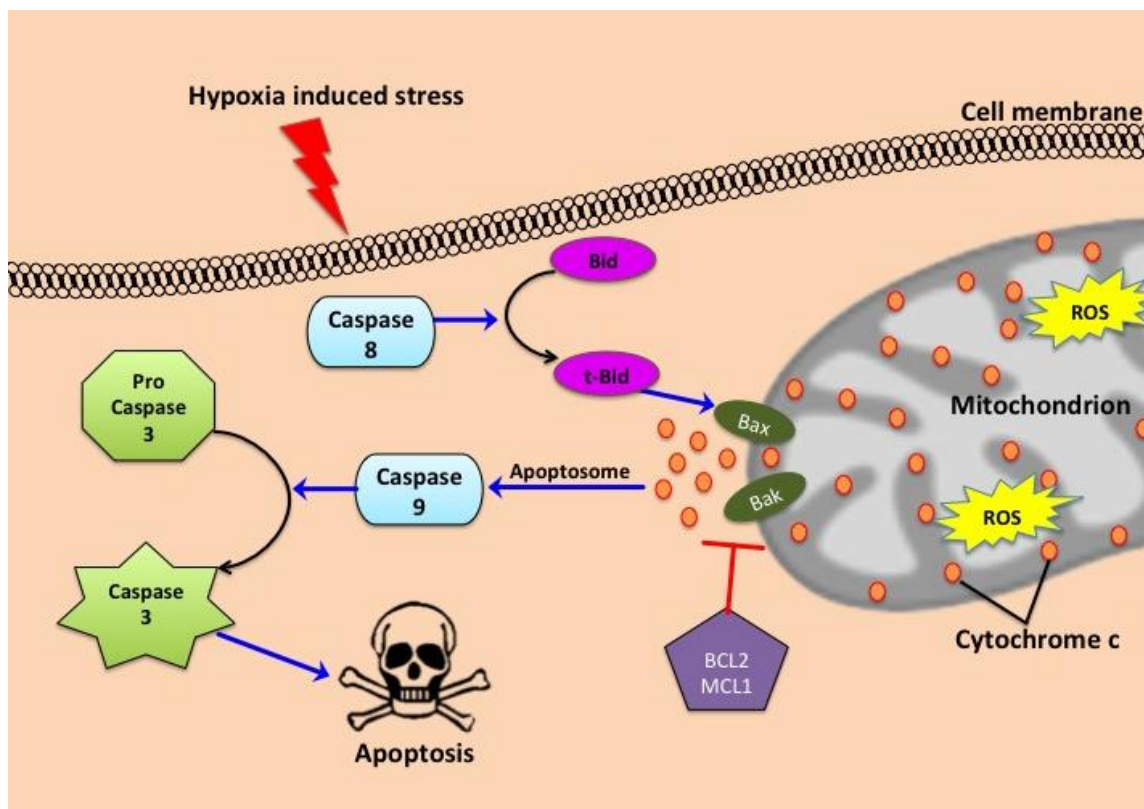


**Figure 1: Mitochondria associated apoptotic pathway.**

Representative image showing the role played by pro-apoptotic and anti-apoptotic molecules in apoptosis. The process can be initiated in the cells by hypoxia-induced stress that initiates the signaling pathway resulting in the activation of pro-caspase-3. The activated caspase-3 finally triggers apoptosis. (ROS – reactive oxygen species).<sup>54-57</sup>

## 1.4 Gasotransmitter family

Living beings contain a wide variety of signaling molecules ranging in size and chemical properties. They can be proteins, lipids, amines, or even gases. A gasotransmitter is defined as a gaseous messenger molecule that can activate a signaling process at the cellular level. For classification purposes, it must meet the conditions listed in Table 1 to qualify as a gasotransmitter.<sup>58</sup> Currently, there are three known members of the gasotransmitter family – nitric oxide (NO), carbon monoxide (CO) and hydrogen sulfide (H<sub>2</sub>S).

**Table 1. Criteria for classification of a gasotransmitter**

1	They are small molecules of gas, like nitric oxide (NO) carbon monoxide (CO) and hydrogen sulfide (H <sub>2</sub> S).
2	They are freely permeable through the membrane and their effects do not depend on membrane receptors.
3	They are endogenously and enzymatically generated in a regulated manner.
4	They have well-defined specific functions at physiologically relevant concentrations
5	Their cellular effects may or may not be mediated by second messengers, but should have specific cellular and molecular targets.

(Modified table from Wang, R.; 2002)

### 1.4.1 Nitric oxide and carbon monoxide

The first gaseous molecule to be classified as a gasotransmitter was NO. It was discovered as an endothelium-derived relaxing factor and macrophage activator.<sup>59</sup> It is produced endogenously during the conversion of L-arginine to L-citrulline by the enzyme nitric oxide synthase (NOS) (Figure 2).<sup>60</sup> There are three subtypes of the NOS enzyme – inducible NOS (iNOS), endothelium NOS (eNOS) and neuronal NOS (nNOS). While the iNOS is triggered during inflammatory conditions and immune responses, the eNOS and nNOS are constitutively expressed in the endothelial cell and neuronal/renal macula densa cells respectively. The physiological role of NO is to modulate platelet aggregation, assist in leukocyte adhesion and smooth muscle relaxation. However, under conditions of hypoxia and in the presence of ROS (such as superoxide ions), NO reacts to form peroxynitrite, which is a strong nitrating oxidant that causes depletion of antioxidants (such as glutathione) and contributes to the I/R damage.<sup>58,60</sup>

CO was known to be formed physiologically long before the analysis of its physiological function.<sup>61</sup> During the conversion of heme to biliverdin by the enzyme heme oxygenase (HO), CO is synthesized by the use of oxygen and energy molecule nicotinamide adenine dinucleotide phosphate (NADP) (Figure 2). Similar to NOS, there are three subtypes for HO – HO-1, HO-2 and HO-3. HO-1 is strongly induced under oxidative, chemical and physical stress in the cortical tubules and renal vasculature; HO-2 is constitutively expressed in the brain while HO-3 is another spliced version of HO-2.<sup>60</sup> At physiological level and concentrations, CO plays anti-stress and anti-inflammatory roles by suppressing the production of inflammatory cytokines<sup>62</sup>, prevents arteriosclerotic lesions<sup>63</sup> and provides cytoprotection by stabilizing hypoxia inducible factor.<sup>64</sup>

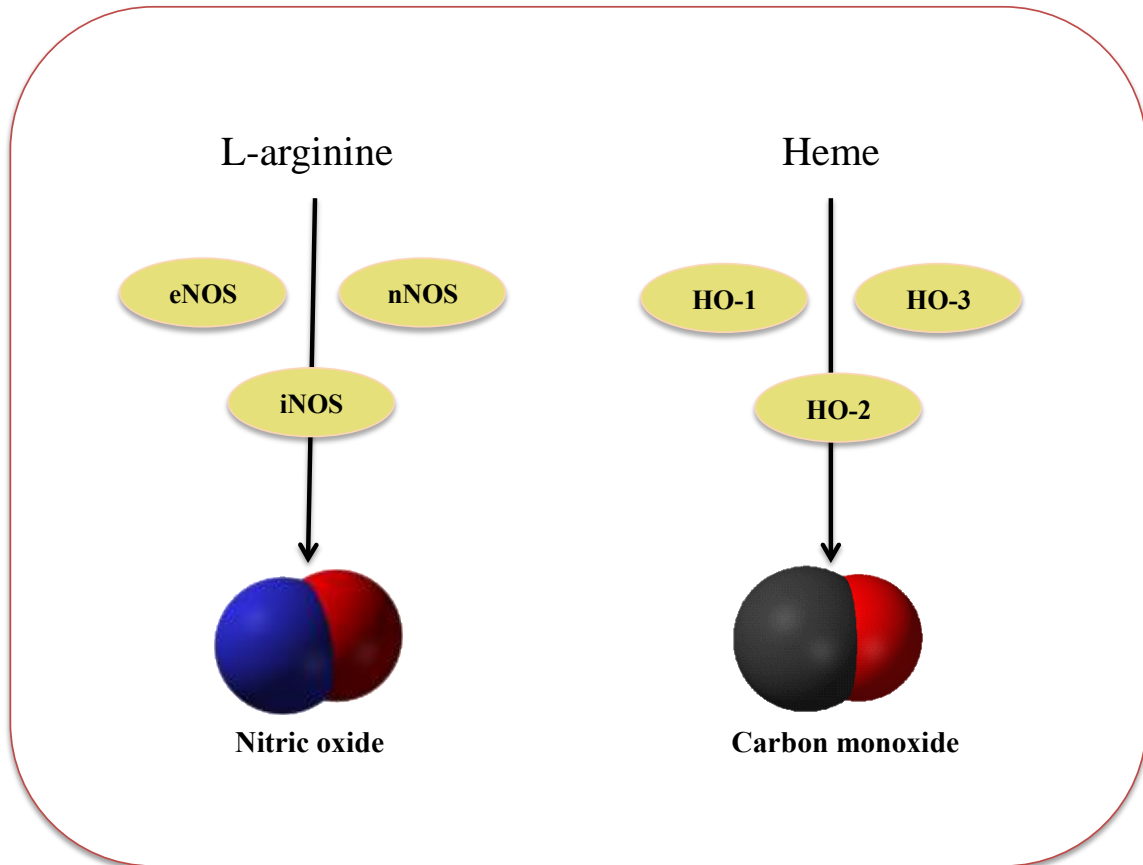


**Figure 2: Endogenous production of NO and CO in cells.**

NO is produced from L-arginine yielding L-citrulline, a reaction catalyzed by three enzymes, nNOS, iNOS and eNOS. The half-life of NO is very short; it is metabolized within milliseconds. CO is produced from heme by HO-1, HO-2 and HO-3. [Modified figure from Snijder *et al.*, 2013]

### 1.4.2 Hydrogen Sulfide

Hydrogen sulfide has been recently added to the family of gasotransmitters.<sup>58</sup> Historically known for its rotten egg smell and toxicity at higher concentrations, it was not until 1989 that H<sub>2</sub>S production was detected endogenously.<sup>65</sup> A few years later, it was proposed to be an endogenous neuromodulator due to its capability of enhancing N-methyl-D-aspartate (NMDA) receptor mediated responses and induction of long term potentiation in hippocampus.<sup>66</sup> Following these discoveries, it was also observed that H<sub>2</sub>S has the capacity to dilate blood vessels in various murine and *in-vitro* models.<sup>67</sup> These characteristics intrigued research interests in the H<sub>2</sub>S molecule.

Non-toxic levels of H<sub>2</sub>S are reported in micromolar quantities as it has been shown to exist at concentrations of 30μM – 300μM in the vertebrate blood.<sup>66,68</sup> In the human body, at a temperature of 37°C and pH of 7.4, 80% of H<sub>2</sub>S exists as a hydrogen sulfite ion (HS<sup>-</sup>).<sup>69</sup> Most mammals produce endogenous H<sub>2</sub>S by using three enzymes - cystathionine gamma lyase (CSE), cystathionine beta synthase and 3-mercaptopyruvate sulfurtransferase (3MST) [Figure 3]. Cysteine is an essential precursor for all of these enzymatic pathways.<sup>66,70</sup> In the kidneys, all three enzymes are primarily located in the proximal tubules in the renal cortex. While CBS and CSE are present in the cytosol of the cells, 3-MST is located in mitochondria as well as cytosol.<sup>71</sup> In fact, these enzymes tend to relocalize to the mitochondria during stress conditions.

Physiologically, the H<sub>2</sub>S plays an important role in preventing inflammation<sup>72</sup>, oxidative stress<sup>73</sup>, neuromodulation<sup>66</sup>, vasoregulation<sup>74</sup> and inhibition of insulin resistance<sup>75</sup>. Further studies in animal models and human disease have shown that defective or less than optimal endogenous H<sub>2</sub>S production causes ageing<sup>76</sup>, cardiovascular diseases<sup>77</sup> and respiratory pathologies like asthma<sup>78</sup> and chronic obstructive pulmonary disease.<sup>79</sup> In addition, involvement of H<sub>2</sub>S in cell functioning, cytoprotection and cellular signaling is being actively explored.

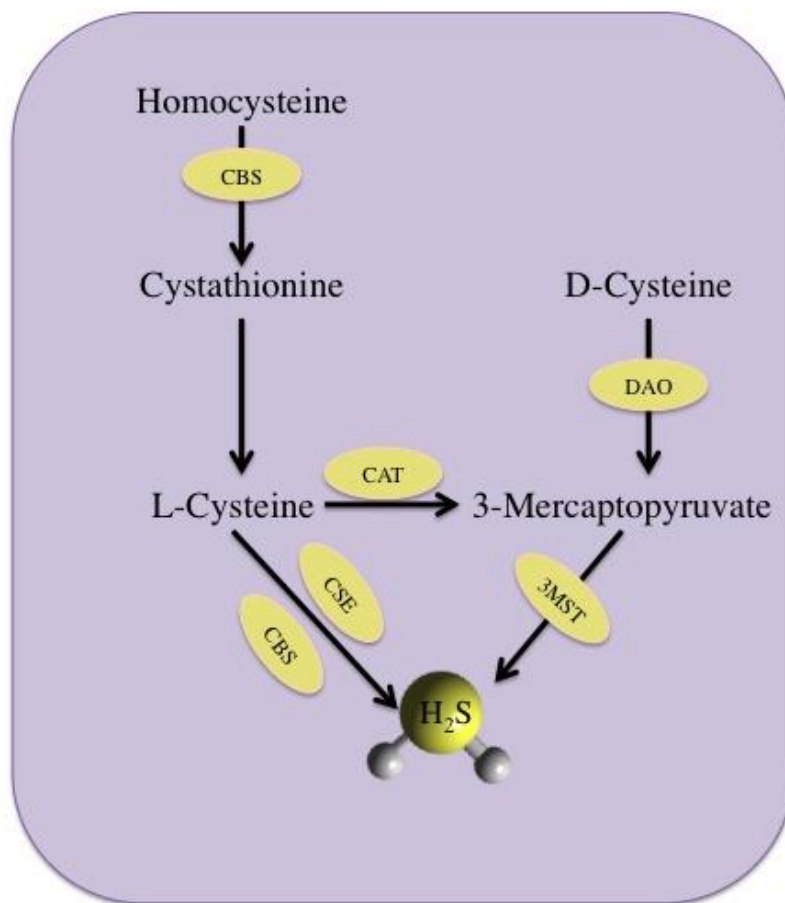


**Figure 3: Enzymatic pathway for endogenous production of hydrogen sulfide.**

H<sub>2</sub>S is produced by CSE, CBS and 3MST from homocysteine, cystathionine, L-cysteine and D-cysteine. Cysteine aminotransferase (CAT) and D-amino acid oxidase (DAO) are required to convert L-cysteine and D-cysteine into 3-mercaptopyruvate (3MP) that is used as a substrate for H<sub>2</sub>S production by 3-MST.[Modified from Snijder *et al.*, 2013]

## 1.5 Hydrogen sulfide and IRI

Numerous studies using *in-vivo* and *ex-vivo* models have demonstrated protective effects of H<sub>2</sub>S against IRI in various organ transplant models including that of the lung<sup>80</sup>, liver<sup>81</sup>, heart<sup>82,83</sup> and kidney.<sup>84,85</sup> The protection rendered by H<sub>2</sub>S in these studies is related to the physiological effects of H<sub>2</sub>S that are discussed in depth in the next section.

### 1.5.1 Inflammation and H<sub>2</sub>S

Inflammation is a protective physiological reaction of vascularized tissue to injury and can be categorized as acute or chronic, depending on the duration and mechanism of the reaction.<sup>86</sup> Acute inflammation is the early host response that results in increased blood flow (vasodilation) and neutrophil infiltration to the site of injury, while chronic inflammation is of prolonged duration and may follow acute inflammation.<sup>87</sup>

H<sub>2</sub>S plays opposing roles in inflammation. Some studies claim that H<sub>2</sub>S helps reduce the inflammatory processes while others show increased inflammation after use of H<sub>2</sub>S. However, the crucial fact that plays an important role in determining the impact of H<sub>2</sub>S on inflammatory processes is its concentration in that tissue or cell. Time and again, it has been shown that higher doses of H<sub>2</sub>S are toxic, pro-inflammatory and cause cell death<sup>88</sup> while lower physiological doses render protection from cell death.<sup>72,74,82</sup>

Some studies have linked the decreased expression of pro-inflammatory molecules as one of the mechanistic pathways of protective H<sub>2</sub>S. An *in-vivo* study has shown a reduction in expression of tumor necrosis factor-alpha (TNF-  $\alpha$ ) following supplementation with H<sub>2</sub>S.<sup>90</sup> TNF-  $\alpha$  is a key member of the cytokine family. It plays a role in immune system during inflammation, cell proliferation, differentiation and apoptosis.<sup>91</sup> Many cell types produce this factor (T-cells, B-cells, neutrophils, etc.) following a stimulation by other cytokines or pathophysiological conditions.<sup>92</sup> A study on human coronary endothelial cells has showed that TNF-  $\alpha$  indirectly contributes to the ROS production in the sites of inflammation<sup>93</sup> and caspase activation leading to apoptosis.<sup>94</sup> Thus, reduction in TNF-  $\alpha$  can help mitigate some harmful effects of IRI.

### 1.5.2 Antioxidant effect

ROS are produced in limited quantities under normal physiological conditions. As a result, the cells are easily able to detoxify the ROS by using specific enzymes such as glutathione peroxidase and superoxide dismutase; and other antioxidant molecules like glutathione and vitamins C & E.<sup>95</sup> Glutathione is one of the most effective antioxidants present in our body. However, when ROS are produced in excess amount during IRI, they can damage the cell membrane and proteins; activate signaling pathways such as mitogen activated protein kinases (MAPK) and c-Jun-N-terminal kinase leading to apoptosis.<sup>96</sup>

H<sub>2</sub>S has been shown to have direct and indirect antioxidant properties. It acts as a direct antioxidant by reducing reactive molecules and scavenging ROS radicals and anions.<sup>97,98</sup> Indirectly, H<sub>2</sub>S is known to up-regulate intracellular levels of glutathione and superoxide dismutase and thereby help in the removal of excessive ROS.<sup>83</sup> *In-vitro* studies by Whiteman *et al.* on human neuro-epithelium cells have depicted reduced lipid peroxidation along with decreased cytotoxic effects of radical and non-radical intermediates (such as peroxynitrites and lipid hydro-peroxides) on protein nitration and oxidation upon treatment with H<sub>2</sub>S.<sup>99,100</sup> Another study by Geng *et al.* also demonstrated protective effect of H<sub>2</sub>S on contractile activity of cardiac myocytes in rats by directly scavenging oxygen free radicals (superoxides and hydrogen peroxides) along with decreasing the accumulation of lipid peroxidations.<sup>101</sup>

### 1.5.3 Protecting mitochondrial integrity and anti-apoptotic role

During oxidative stress conditions, excessively produced ROS and calcium ions accumulate in the mitochondria as some of the ion channels fail to function properly in the absence of ATP.<sup>50</sup> The hypoxic stress also causes depolarization of the mitochondrial membrane<sup>52</sup> (discussed previously under “IRI effects at cellular level”). The MMPT eventually causes the breakdown of the mitochondria and the cell can no longer survive without the energy (ATP) to fuel its metabolism. *In-vitro* and *in-vivo* studies have shown that H<sub>2</sub>S treatment results in improvement of mitochondrial respiration recovery rate, increased efficacy of complex I&II and reduced mitochondrial swelling following IRI.<sup>83</sup> It also helps to scavenge the ROS present in the mitochondria by up regulating



glutathione and superoxide dismutase. Overall, H<sub>2</sub>S protects mitochondrial degradation/breakdown due to IRI.

Studies have also reported the protective effects of H<sub>2</sub>S against apoptosis. In a murine model of oxidative stress related to hemorrhagic shock, Xu *et al.* demonstrated that H<sub>2</sub>S administration protected the lungs by suppressing oxidative stress and apoptotic signaling pathway along with decreasing the expression of various mitochondria associated and other apoptotic proteins such as active caspase 3/8, Bax and increased expression of anti-apoptotic protein Bcl-2. Another study by Sivarajah *et al.* showed that H<sub>2</sub>S is associated with decreased apoptosis demonstrated by reduction in caspase 9 activity in the cardiac myocytes subjected to 25 minutes of ischemia and 2 hours of reperfusion in a rat model.<sup>104</sup> Based on these studies, H<sub>2</sub>S seems to down regulate the proteins associated with apoptosis while up-regulating the ones that prevent cell damage and death.

#### 1.5.4 H<sub>2</sub>S donor molecules

H<sub>2</sub>S exists as a gaseous form of matter. This physical property limits the use of this form since it would be hard to deliver and maintain accurate dissolved concentration of a gas. As a result, a variety of H<sub>2</sub>S donor molecules are being used to study the effects of H<sub>2</sub>S supplementation through *in-vivo* or *in-vitro* IRI models.

Some of the natural compounds that are most commonly used to deliver H<sub>2</sub>S in research setting include salts like sodium hydrogen sulfide or sodium sulfide (NaHS/ Na<sub>2</sub>S), L-cysteine and D-cysteine. While the crude sulfide salts provide exogenous H<sub>2</sub>S, the different isomers of cysteine help with the endogenous production of H<sub>2</sub>S. L-cysteine has been long known to contribute to endogenous production of H<sub>2</sub>S through the use of CBS, CSE and 3-MST enzymes. D-cysteine has only been recently identified as a novel pathway for endogenous H<sub>2</sub>S production via the use of DAO and 3-MST enzymes. However, the D-cysteine involving pathway is optimal at physiological pH 7.4 and independent of two pyridoxal 5'-phosphate (PLP) unlike the L-cysteine pathway that prefers alkaline pH and is PLP dependent. In addition, the D-cysteine has 80 fold greater H<sub>2</sub>S producing activity in the kidneys than the L-cysteine.<sup>105</sup> Furthermore, the study by Shibuya *et al.* has demonstrated more efficient protection against IRI in the renal cortex

of mice following oral administration of D-cysteine in comparison to L-cysteine.<sup>106</sup> This makes D-cysteine a better choice over L-cysteine for increasing the endogenous production of H<sub>2</sub>S.

Although the sulfide salts (NaHS, Na<sub>2</sub>S) are readily available and convenient to use in laboratory, Whiteman *et al.* has listed a few drawbacks associated with the use of these molecules as H<sub>2</sub>S donors.<sup>107</sup> First of all, salts like NaHS/ Na<sub>2</sub>S undergo instantaneous dissociation that generates H<sub>2</sub>S gas. The rapid dissolution causes a burst of the gas that could also lead to toxicity in the cell considering the basal plasma levels of H<sub>2</sub>S in vertebrates have been reported to be around 30µM to 300µM and the concentration of sodium sulfide salts used in research studies ranges from high micromolar to millimolar concentrations. In contrast, the endogenous enzymatic production of H<sub>2</sub>S is a slow and sustained process carried out by CBS, CSE and 3-MST.<sup>60</sup> Further, the problem of zero sustainability of H<sub>2</sub>S release renders the cells susceptible to injury in the subsequent phases of IRI.

These drawbacks prompted the search for slow releasing H<sub>2</sub>S donors that could continue releasing H<sub>2</sub>S over longer periods of time. This would also help to lessen the chances of toxicity since only limited amount of H<sub>2</sub>S is released in a given time. Moore and colleagues, at the National University of Singapore, developed the first water soluble slow-releasing H<sub>2</sub>S donor named as morpholin-4-ium 4 methoxyphenyl(morpholino) phosphinodithioate (GYY4137).<sup>108</sup> The chemical synthesis equation is shown in figure 4 and depicts the molecular structure of the molecule. In their study, it was observed that GYY4137 takes about 600 seconds to reach its peak rate of release and then maintains the release rate for over 180 minutes. This particular feature enables it to mimic the biological conditions where a sustained release of H<sub>2</sub>S is available to the cells when needed. Also, it should be noted that every molecule of GYY4137 releases two molecules of H<sub>2</sub>S and the decomposition products of this molecule seem to be inactive with no possible effects on the cells.<sup>87</sup> Further, the final concentrations of H<sub>2</sub>S generated from GYY4137 are more physiologically, pathophysiologically and therapeutically relevant than those from the sulfide salts. Lastly, the water solubility of GYY4137 makes it very convenient for use in laboratory as it can be easily dissolved in water based solvents (cell culture medium as

well) without requiring specific organic solvents such as the dimethyl sulfoxide (DMSO).<sup>109</sup>

A review of literature shows very similar protective effects of GYY4137 as the H<sub>2</sub>S molecule. As described previously, H<sub>2</sub>S plays a role in decreasing oxidative stress and preserving mitochondrial membrane potential during IRI. Likewise, GYY4137 has been shown to exert cytoprotective effects in cellular and animal models. For instance, 10μM - 200μM dose range of this molecule impedes cytotoxicity induced by H<sub>2</sub>O<sub>2</sub> and peroxynitrite in human mesenchymal progenitor cells and human articular chondrocytes. In the same study, it was shown to preserve mitochondrial membrane potential and inhibited ROS production in the mitochondria.<sup>110</sup> Furthermore, a study on human umbilical vein endothelial cells (HUVEC) substantiated the role played by endogenous H<sub>2</sub>S in suppressing the cytotoxicity induced by H<sub>2</sub>O<sub>2</sub> whereby the siRNA-mediated knockdown of CSE aggravated cellular injury.<sup>111</sup> This supports the viable notion of therapeutic capability for H<sub>2</sub>S donor molecules.

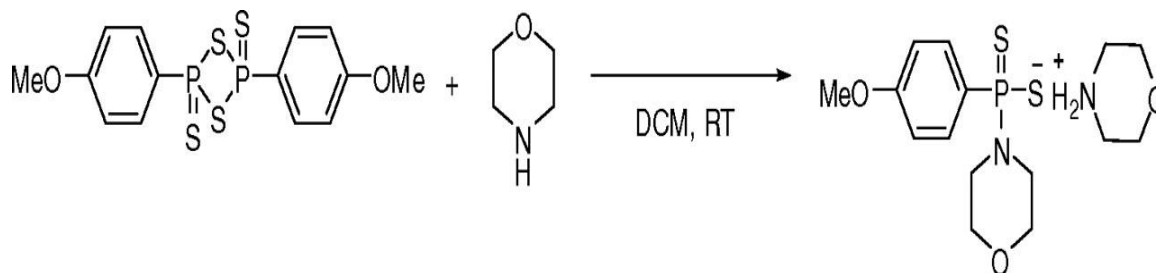


**Figure 4: Chemical equation for synthesis of GYY4137**

Morpholine [20mmol] (dissolved in methyl chloride) was added to of 2,4-bis(4-methoxyphenyl)-2,4-dithioxo-1,3,2,4-dithiadiphosphetane [4mmol] (dissolved in methyl chloride) in the presence of dichloromethane (DCM) at room temperature (RT). (Taken from Li *et al.*, 2008)

## 1.6 Rationale, Hypotheses and Aims

### 1.6.1 Rationale

Our lab has previously shown that supplementation of organ preservation solution with H<sub>2</sub>S leads to significant survival and tissue protection at prolonged periods of cold ischemic stress (24 hours) followed by subsequent renal transplantation.<sup>112</sup> We have also observed that H<sub>2</sub>S renders protection against warm renal IRI in a non-transplantation model of uni-nephrectomised rats involving 1 hour warm ischemia and 2 hours of reperfusion.<sup>90</sup> Although numerous studies have shown the protective effects of H<sub>2</sub>S against renal IRI, not a lot has been explored in the field of DCD transplants that involve a combination of warm and cold ischemia. Through this study, I aimed to assess the protective effects of H<sub>2</sub>S supplementation in a murine model of DCD transplantation and further assess the mechanisms underlying the protective role of H<sub>2</sub>S in such a model.

### 1.6.2 Hypotheses

#### *In-vivo*

Supplementing donor rats with a precursor H<sub>2</sub>S molecule and the cold organ preservation solution (UW) with exogenous H<sub>2</sub>S would accelerate renal recovery and improve graft function along with the recipient survival rates.

#### *In-vitro*

Addition of synthetic H<sub>2</sub>S donor molecule during hypoxia to the growth media of porcine kidney proximal tubular epithelial cells (LLC-PK1) would help attenuate pathophysiological effects of IRI at cellular level resulting in increased cell viability.

### 1.6.3 Aims

**Aim 1:** To compare renal function in the treatment and untreated group recipient rats by analyzing serum and urine samples

**Aim 2:** To assess the renal graft obtained at end point or after death of the subject for apoptosis and glomerular/tubular necrosis using histological staining techniques (TUNEL stain & H/E stain)

**Aim 3:** To measure mRNA expression of various pro-inflammatory (TNF-  $\alpha$ ), pro-apoptotic (Bax, Bid) and anti-apoptotic (Bcl-2] mediators

**Aim 4:** To understand the underlying mechanism for protective effects of H<sub>2</sub>S using an *in-vitro* model

Aim 4.1: Develop a protocol for the *in-vitro* IRI model

Aim 4.2: Study and quantify effect of GYY4137 on cells exposed to hypoxia and subsequent reoxygenation by measuring necrosis, late apoptosis and cell viability

Aim 4.3: Assess the effect of H<sub>2</sub>S supplementation on mitochondrial apoptotic pathway by measuring changes in ROS, mitochondrial membrane potential and changes in expression of mitochondria associated apoptotic markers

## Chapter 2

### 2 Materials and Methods

This section describes the different methods that were used to carry out the experiments covered under this project. It involved the use of both *in-vivo* and *in-vitro* methods.

#### 2.1 Murine Model of Donation after Cardiac Death (DCD) Renal Transplantation

##### 2.1.1 Animal description and care

Adult male Lewis syngeneic rats (250g – 300g) purchased from Charles River Laboratories International Limited (USA) were used for this study to prevent any confounding effects of immunosuppression. The animals were maintained in accordance with the Committee on Care and Use of Laboratory Animals of the Institute of Laboratory Animal Resources, National Research Council. The animals were housed at the animal facility located in the Animal Care and Veterinary Services Department at The University of Western Ontario. The experimental protocol and housing conditions followed the guidelines of the Council on Animal Care of the institution.

##### 2.1.2 Preliminary experiments and final experimental design

The rats were randomly divided into one of the following three groups: sham, untreated or treatment. The sham group rats underwent a midline incision and the procedure did not involve kidney transplantation. On the other hand, the untreated and the treatment group rats received the donor kidneys that had experienced a combination of warm and cold ischemic injury.

To decide the time intervals for warm and cold ischemia, some preliminary experiments were carried out. In the beginning, prolonged warm (45 minutes) and cold ischemic (18 hours) times were used to maximize the amount of injury and to see a better difference between the untreated and treatment groups. However, the recipient rats were unable to survive past post-operative day two in both the groups. Thereafter, the warm ischemic injury time was lowered to 20 minutes while maintaining the same cold ischemic time so

as to make sure the grafts retained their function in the recipient. Due to the reduced injury to the donor kidney, the rats in both groups survived until the end point of 30 days. The serum creatinine levels showed slight differences between the untreated and the treatment group such that there was a faster recovery of renal function in the treatment group (Appendix A). However, the warm ischemia time did not appear to cause significant injury to the grafts as both the treatment and the untreated group recipients were able to recover from the induced injuries and survived until the end point.

In the finalized experimental design (shown in Figure 5), the warm ischemic time was increased to 30 minutes and the cold ischemic time was 18 hours so as to cause sufficient damage to observe significant differences between the different experimental groups. The untreated and treatment group rats received the donor kidneys that had undergone clamping for 30 minutes and a cold storage period of 18 hours in the standard organ preservation solution called University of Wisconsin (UW) solution. The main differences between the untreated and the treatment group included injecting the donor rats with D-cysteine prior to the surgical procedure and supplementing the organ storage and flush solution with hydrogen sulfide (H<sub>2</sub>S) as detailed in section 2.1.3.

### 2.1.3 Surgical procedure

The donor rats for the treatment group received an intraperitoneal (I.P.) injection of D-cysteine (purchased from Sigma Aldrich Company, USA) dissolved in 0.5mL of sterile saline solution (0.9%NaCl) at a concentration of 2mmol/kg rat weight at least one hour prior to the clamping of the pedicle. The dosage and timing for D-cysteine injection was based on a study by Shibuya *et al.* where he orally administered D-cysteine at a dose of 8mmol/kg of the body weight of mice and observed increased concentrations of H<sub>2</sub>S in those mice for up to 3 hours following ingestion.<sup>106</sup> Taking into account the lower gastrointestinal absorption of the ingested drug, the donor rats were injected intraperitoneally with D-cysteine at 4mmol/kg body weight in our pilot experiment. However, none of the treatment rats survived in that experiment. Therefore, the dosage of D-cysteine was reduced to half that amount (2mmol/kg of rat weight) in our preliminary experiments and the treatment rats were able to survive following renal transplantation.



The rats were anesthetized by intramuscular injection of 0.2ml ketamine/xylazine and maintained under anesthesia with 2% isoflurane during surgery. In donor rats, the left renal pedicle was occluded via atraumatic clamping for 30 minutes to induce warm ischemia. The left kidney was then flushed with 5mL of UW solution and procured. Following procurement, it was stored in 50mL of the same solution at 4°C for 18 hours to encounter cold ischemia. However, the UW flush and storage solution was supplemented with 150µM NaHS (sodium hydrogen sulfide) for the treatment group. The same dose (150µM NaHS) was also used in our other *in-vivo* IRI study in a rat model that involved extended periods of cold ischemic stress and showed beneficial effects.

The recipient syngeneic Lewis rats underwent bilateral nephrectomy followed by renal transplantation of the left kidney procured from the donor. Each surgery was performed by the same experienced micro-surgeon (Dr. Jifu Jiang, Microsurgeon, Matthew Mailing Centre for Translational and Transplantation studies) who was blinded to the treatment group. The length of the surgery/operating time was similar for the untreated and the treatment group.

#### 2.1.4 Post-operative monitoring

The recipient animals were monitored for a period of 30 days or until the time of death (whichever came first). Daily health records were maintained for these animals. No surgical complications were caused by the anastomoses that were carefully examined at the time of death or sacrifice. Blood and urine samples were obtained from these rats on post-operative days 3,5,10,20 and 30. The rats were placed in metabolic cages to collect urine while the blood samples (500µL) were taken from the tail vein. The blood was centrifuged at 12,000g for 5 minutes to separate the serum. The serum and urine samples were then stored at -20°C for later analysis.

#### 2.1.5 Assessment of graft renal function and injury

Serum obtained from the blood samples was analyzed at Core Pathology Laboratories (University Hospital, London Health Sciences Centre) for creatinine, urea and osmolality. The urine samples were also examined for creatinine and protein at the same lab facility. The creatinine and protein values from the urine samples were used to calculate the urine

protein-creatinine ratio (adjusted to the rat weight) as an indication of any prevalent signs of proteinuria in the recipients. The urine osmolality was measured in the lab using The Advanced<sup>®</sup> Micro-Osmometer Model 3320 (Advanced Instruments Inc., Massachusetts, USA). Basically, 20 $\mu$ L of the sample was loaded into the sampler tip of the plunger and then inserted into the sample port. The test was run for approximately one minute and the readings were collected. In case of multiple samples being tested on the same day, sample port was cleaned properly before switching between samples. Also the first readings for the successive samples, following the first sample, were discarded and the second reading was recorded to prevent any errors due to sample contamination.

### 2.1.6 Renal histopathology

At the time of death or sacrifice, the kidney grafts were removed and bivalved sagittally such that one half was stored at -80°C and used for qRT-PCR analysis while the other half was used for histological staining. The tissues were fixed in 10% formalin and sent to the Molecular Pathology Core Facility (Robarts Research Institute, London, Canada) for processing. The tissues were embedded, sectioned (8 $\mu$ m width) and stained with hematoxylin and eosin (H&E) to detect any signs of necrosis. All H&E sections were analyzed and quantified by an experienced clinical renal pathologist (Dr. Aaron Haig, London Health Sciences Centre) who was blinded to the treatment assignments. The slides were scored for acute tubular necrosis (ATN) on a scale of 0-5; where 0 represents absence, 1 denotes involvement of 1%-10% of glomeruli or cortical area, 2 is 11% - 25%, 3 is 26% - 45%, 4 is 46% - 75% and 5 is greater than 75%.

The histological sections also underwent terminal deoxynucleotidyl-transferase-mediated dUTP nick end labeling (TUNEL) to determine the level of apoptosis. All slides were analyzed by taking five pictures of random slide sections per sample using Nikon microscope at 10X magnification. The injury in the images was assessed using Image-J software by formulating a macro to precisely identify the dark stained cells in the slides. The total cell count for each picture was recorded and the median (from five pictures) was used to denote each sample.

### 2.1.7 RNA isolation, cDNA synthesis and real time PCR

The rats that had either died or were sacrificed by post-operative day 3 for each of the sham, untreated and treatment groups were used to look at relative *mRNA* expression levels for certain inflammation and apoptosis related genes. A small part of renal tissue (containing both the cortex and medulla) measuring one gram in mass was cut from the sagittally bivalved kidney stored at  $-80^{\circ}\text{C}$ . It was thawed and immediately homogenized using a mechanical homogenizer and simultaneously adding cell disruption buffer (provided in the PARIS kit). The homogenate was placed on ice the whole time (including the time when it was being homogenized) to prevent any degradation of the *mRNA* or proteins. The total RNA content was isolated from the homogenate using Protein and RNA (PARIS) Isolation kit (life technologies, USA) as per the manufacturer's protocol. Briefly, equal volumes ( $200\mu\text{L}$ ) of cell lysis buffer (PARIS kit) and 100% ethanol were added to  $200\mu\text{L}$  of tissue homogenate. The entire mixture ( $600\mu\text{L}$ ) was centrifuged at  $12000\times g$  for 1-2 minutes in a collection tube with filter. The filtrate was discarded and the filter was washed sequentially with wash buffer 1 (one time) and wash buffer 2/3 (two times). The *mRNA* was recovered using the elution buffer (heated to  $95^{\circ}\text{C}$ ) with two sequential dilutions of  $40\mu\text{L}$  and  $10\mu\text{L}$ . All the buffers were provided with the PARIS kit. For reverse transcription,  $4\mu\text{L}$  of SuperScript VILO™ MasterMix (Invitrogen) was added to about 400ng of *mRNA* and the sample volume was normalized to  $20\mu\text{L}$  by addition of DEPC treated water (0.1% DEPC). The sample tubes were then placed in the Eppendorf thermal cycler set to the following cycles:  $25^{\circ}\text{C}$  (10 minutes),  $42^{\circ}\text{C}$  (60 minutes) and  $85^{\circ}\text{C}$  (5 minutes). After completion of the cycles, the *cDNA* samples were stored at  $4^{\circ}\text{C}$ . The concentration and quality of the isolated *mRNA* and *cDNA* were analyzed using NanoDrop 2000. The  $A_{260/280}$  readings for the isolated *mRNA* and *cDNA* were consistently greater than 1.8 indicating little to no contamination.

For qPCR, each sample used 2x SensiFAST SYBR Hi-ROX Mix (BIOLINE) and had a total volume of  $20\mu\text{L}$  containing 20ng of respective *cDNA*. The forward and the reverse primer sequences were generated using the NCBI database and the IDT primer quest tool. The primers were ordered from Sigma Aldrich and the primer sequences are provided in table 3. The target gene signals were normalized against  $\beta$ -actin. All qRT-PCR assays

were performed using *BIO-RAD* thermal cycler and software package and the results were analyzed using Graph pad prism 6.

### 2.1.8 Data analysis

The data were analyzed using the Graph Pad prism 6 software. All statistical analyses involved use of either one-way or two-way ANOVA (with multiple comparisons) or Student's t-tests (multiple) as required and the survival analysis was done using the Kaplan-Meier method. Statistical significance was accepted at  $p < 0.05$  with a confidence interval of 95%. The values reported in results section (all figures) are mean  $\pm$  standard error mean (SEM) unless otherwise stated.

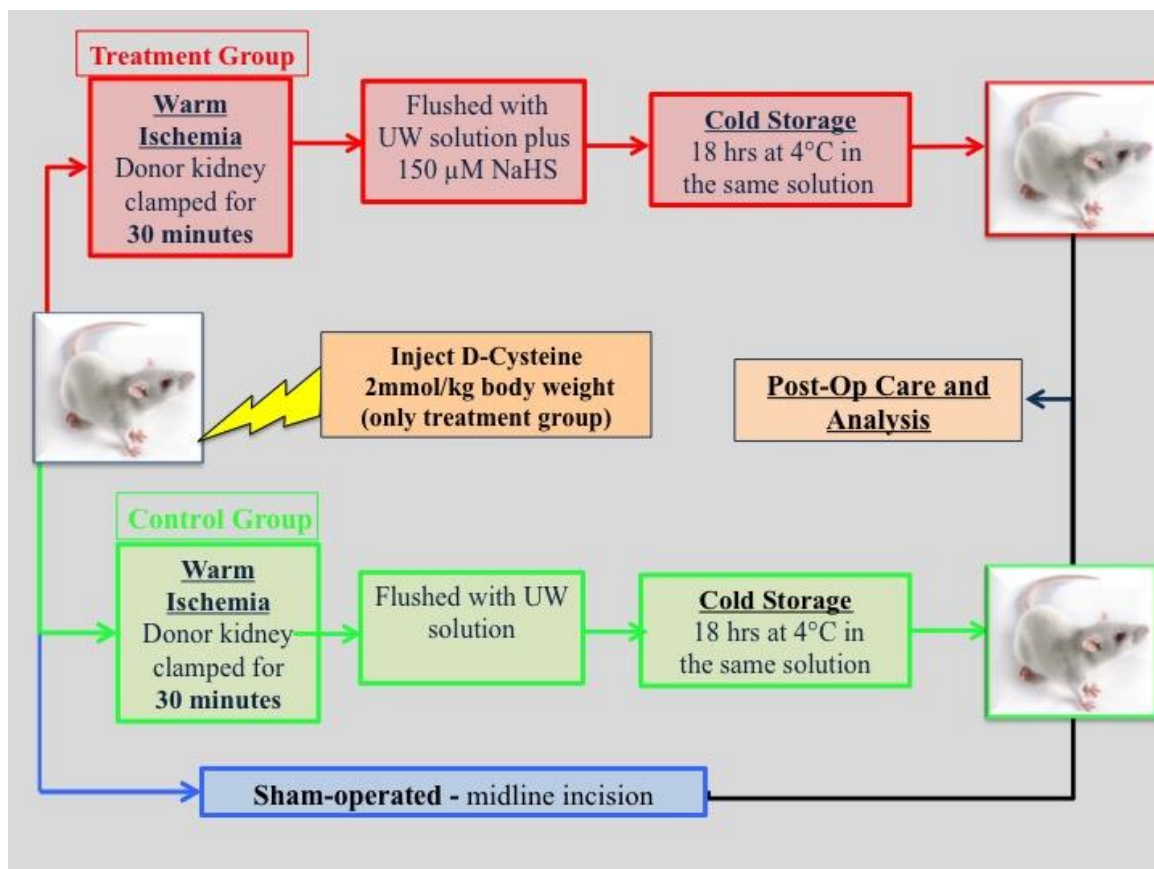


**Figure 5: Finalized experimental design for *in-vivo* murine model of DCD renal transplantation**

The figure shows three experimental groups – the treatment group (red), the untreated group (green) and the sham-operated (blue). The sham group rats only undergo a midline incision. In untreated and treatment groups, the donor rat’s kidney pedicle is clamped for 30 minutes (warm ischemia) and then stored at 4°C (cold storage/ischemia) for 18 hours. D-cysteine is injected intraperitoneally one hour prior to ischemic injury in donor rats and 150 NaHS is added to UW solution only for the treatment group. The recipient rats undergo bilateral nephrectomy prior to the transplantation of the renal grafts and are monitored until the end point (30 days) or the time of death, whichever comes first.

**Table 2. Primer sequences (rat) used in qRT-PCR reactions**

S. No.	Gene	Sequence 5' → 3'
1.	B-actin forward	GTGTGGATTGGTGGCTCTATC
	B-actin Reverse	CAGTCCGCCTAGAAGCATTT
2.	BAX Forward	TGCTACAGGGTTTCATCCAG
	BAX Reverse	GACTCTCGCTCAGCTTCTT
3.	BID Forward	CGATACGGCAAGAATTGTGAAG
	BID Reverse	ATTCCCACCACCTGGAAATAG
4.	Caspase-3 Forward	CCACGGAATTTGAGTCCTTCT
	Caspase-3 Reverse	CCACTCCCAGTCATTCCTTTAG
5.	BCL-2 Forward	GTGGATGACTGAGTACCTGAAC
	BCL-2 Reverse	GAGACAGCCAGGAGAAATCAA
6.	TNF $\alpha$ Forward	GCAGATGGGCTGTACCTTATC
	TNF- $\alpha$ Reverse	GAAATGGCAAATCGGCTGAC

## 2.2 DCD model in LLC-PK1 cells

### 2.2.1 LLC-PK1 cell line

The proximal tubular epithelial pig kidney cell line (LLC-PK1) was used for the *in-vitro* experiments. These cells were obtained in a frozen vial from the American Type Culture Collection (ATCC, Rockville, MD, USA). The cells were cultured in 75cm<sup>2</sup> flasks in a carbon-dioxide incubator (5% CO<sub>2</sub>) at 37°C using Medium199 (M199; Life Technologies Inc., USA) that contained penicillin (100 U/mL), streptomycin (100 U/mL) and was supplemented with 10% heat-inactivated fetal bovine serum (FBS; Hyclone, Logan, USA). The cells were sub-cultured and plated onto twelve well plates upon reaching 80% - 90% confluence.

### 2.2.2 Synthetic hydrogen sulfide donor used

For the *in-vitro* experiments involving hypoxic injury, slow releasing synthetic hydrogen sulfide donor GYY4137 (courtesy of Dr. Matthew Whiteman from Exeter Medical School, England) was used to study the mechanism of hydrogen sulfide protection at a cellular level. Studies have shown that it reaches its peak rate of release approximately 600s later than sodium hydrogen sulfide. Also, this molecule tends to maintain its peak release rate over a longer period of time rather than an initial burst observed in case of sodium hydrogen sulfide salts.

### 2.2.3 Experimental design

For all *in-vitro* experiments,  $2 \times 10^5$  cells suspended in 1mL of Medium199 (10%FBS, 1% Penicillin/Streptomycin) were plated in each well in the 12-well plate and allowed to grow in the carbon-dioxide incubator for 36 hours. During the experimental conditions, Dulbecco's Modified Eagle's Medium (DMEM; without any glucose or FBS) was used to restrict the supply of nutrients to the cells. Upon reaching 80% - 90% confluence, hydrogen sulfide donor molecule (GYY4137) dissolved in DMEM at varying concentrations (500nM – 500µM) was added to the wells. The plates were then placed in the hypoxia chamber (H85 Whitley hypoxy-station) set to 1% oxygen, 5% carbon dioxide and 94% nitrogen thereby limiting oxygen supply to mimic the conditions experienced

during ischemic injury. For warm conditions, the temperature of the hypoxia chamber was set to 37°C while for the cold conditions the lowest internal temperature achieved in the chamber was 7°C – 8°C and the 12 well plates had to be placed on ice packs to reach temperature of 4°C. A thermometer was placed beside the plates on the ice pack to verify the temperature experienced by the cells.

In the beginning, a number of trials were conducted to finalise a combination of warm and cold hypoxic interval that would cause enough damage to the cells thereby lowering their viability by at least 40% - 50%, but at the same time the damage caused had to be reversible such that the cells could be rescued from that damage with the treatments being provided. These combination times included 3 hours warm + 3 hours cold, 3 hours warm + 9 hours cold, 4 hours warm + 6 hours cold and 4 hours warm + 8 hours cold (Figure 12). In all these combination experiments, it was observed that the ischemic injury (as measured by the percentage of viable cells) did not change by a large extent with the increases in the cold hypoxic time but depicted some change when the warm hypoxic time was increased. In order to see a significant difference in rescue, the hypoxic time was further increased and the percentages of viable cells were compared between the following hypoxic treatments: 12 hours warm + 24 hours cold and 12 hours warm (only). Based on the results (as described in the result section), the future experiments were conducted with the 12 hours of warm hypoxic time.

#### 2.2.4 Viability analysis

After experiencing 12 hours of warm hypoxic time, the 12 well plates were taken out of the hypoxia chamber. The DMEM (media) from the wells was centrifuged at 500 x g for 5 minutes to collect any floaters or dead cells in it. These dead cells were suspended in 1mL of Medium199 (1% penicillin/streptomycin and 10% FBS) and re-added to the same wells. The plates were placed in the carbon-dioxide incubator (at 37°C, 5% CO<sub>2</sub>) for 24 hours allowing reoxygenation and associated injury.

Following reoxygenation, the cell samples were analyzed for the percentage of viable cells. Briefly, the reoxygenation media was collected in labeled flow tubes. The wells were washed with 1X phosphate buffered saline (PBS) solution to remove any traces of



FBS in the wells and 100µL of 0.25% trypsin (Gibco, Life technologies, USA) was added to each well to lift the monolayer of cells. The plates containing trypsin were incubated at 37°C for 3-6 minutes to accelerate the process. Following incubation, 500µL of medium199 (1%Penicillin/Streptomycin, 10%FBS) was added to the wells to inactivate the trypsin and the medium (now containing the trypsinized cells) was collected in the same flow tubes. Two samples of heat-killed cells (65°C, 10 minutes) were used as positive control for the stains. The flow tubes were then centrifuged at 600 x g for 6 minutes to get a rigid pellet of cells at the bottom. The supernatant was removed and the cells were washed with 1X-PBS two times by re-suspension and centrifugation. The final pellet of cells was suspended in 100µL of Annexin-V binding buffer (Biology Legend, USA). Following suspension, 1µL of PE conjugated Annexin-V (Biology Legend, USA) and 3µL of 7- Aminoactinomycin-D (7-AAD; Bio Legend, USA) stains were added to each tube and allowed to incubate in dark for 15 minutes. The stained samples were then analyzed using the Beckman Coulter FC 500 flow cytometer (Beckman Coulter Canada, ON). Two channels, FL2 with 572BP filter for PE conjugated Annexin-V and FL4 with 675 BP filter for detecting 7-AAD, were used to assess the viability of cell samples.

### 2.2.5 Quantification of reactive oxygen species

The amount of reactive oxygen species was also quantified in the treatments. Briefly, the treatment group (DMEM only, DMEM with 50µM GYY4137) plate was taken out from the hypoxia chamber. The DMEM (cell media) was collected in labeled flow tubes and the wells were re-perfused in medium199 (no phenol red, 10%FBS, 1% P/S) for half an hour in the incubator. Following the re-perfusion, the cells were trypsinized and cell pellet collected using the same procedure and steps used for viability analysis. For the positive control, the cells were suspended in 500µL of 1XPBS containing 3% hydrogen peroxide (H<sub>2</sub>O<sub>2</sub>) for about 10 minutes prior to the collection of cell pellet. The cell pellets were then suspended in 100µL of 1X-PBS and 2µL of 1mM stock dihydrorhodamine 123 (DHR 123, Life technologies, USA) stain was added to each flow tube. The tubes were incubated in the dark for about 15 minutes before being analyzed in the flow cytometer (Beckman Coulter) using FL1 channel.

### 2.2.6 Detection of mitochondrial membrane depolarization

The cell samples were also analyzed for changes in the mitochondrial membrane permeability by using the stain JC-1 (Invitrogen, Life Technologies) for flow cytometry. Following the hypoxic injury (12 hours warm in hypoxia chamber), the media from the wells was collected in the centrifuge tubes and the wells were washed with 1X PBS to remove any traces of media. The cells were then trypsinized (with 0.25% trypsin and 3-5 minutes incubation) and 500 $\mu$ L of medium199 (1% Penicillin/Streptomycin, 10% FBS) was added to the wells to inactivate the trypsin. The medium containing the trypsinized cells was collected in the same flow tubes. A sample of heat-killed cells (65°C, 10 minutes) was used as a positive control for the stain. The flow tubes were centrifuged at 600 x g for 6 minutes to get a rigid pellet of cells at the bottom. The supernatant was removed and the cells were washed with 1X-PBS two times by re-suspension and centrifugation. The final pellet of cells was suspended in 100 $\mu$ L of medium199 and 1 $\mu$ L of JC-1 stain was added to the tubes. The tubes were then placed in the carbon dioxide incubator at 37°C for 15 minutes and analyzed using the FL1 channel on flow cytometer.

### 2.2.7 Measuring mRNA expression of apoptosis related proteins

The total RNA content was isolated from the cells following 15 minutes of reoxygenation with M199 media after 12 hours of warm hypoxia. The wells were washed with 1X PBS twice to remove any traces of media. About 1mL of Ribozol® was added to the each well and allowed to sit for 4-5 minutes. The cell homogenate was passed through the pipette tip 3 times before collecting it in an eppendorf tube. The mRNA was extracted from the homogenate using the Pure Link® RNA Mini Kit (ambion® by Life Technologies, USA). Briefly 700 $\mu$ L of 70% ethanol was added to each tube and centrifuged in the spin cartridge at 12000xg for 15 seconds. The filtrate was discarded and the filter was washed sequentially with wash buffer 1 (one time) and wash buffer 2/3 (two times). The mRNA was finally recovered using the 30 $\mu$ L of RNAase-free water. All the buffers were provided with the kit. For reverse transcription, 4 $\mu$ L of SuperScript VILO™ MasterMix (Invitrogen) was added to about 300ng of mRNA and the sample volume was normalized to 20 $\mu$ L by addition of DEPC (0.1%) treated water. The sample tubes were then placed in the Eppendorf thermal cycler set to the following cycles: 25°C (10 minutes), 42°C (60

minutes) and 85°C (5 minutes). After completion of the cycles, the *cDNA* samples were stored at 4°C. The concentrations of the isolated *mRNA* and *cDNA* were measured using nanodrop. The  $A_{260/280}$  readings for the isolated *mRNA* and *cDNA* were consistently greater than 1.8 indicating little to no contamination.

For qPCR, each sample used 2x SensiFAST SYBR Hi-ROX Mix (BIOLINE) and had a total volume of 20 $\mu$ L containing 20ng of respective *cDNA*. The forward and the reverse primer sequences were generated using the NCBI database and the IDT primer quest tool. The primers were ordered from Sigma Aldrich and the primer sequences are provided in table 4. The target gene signals were normalized against  $\beta$ -actin. All qRT-PCR assays were performed using *BIO-RAD* thermal cycler and software package and the results were analyzed using Graph pad prism 6.

### 2.2.8 Data analysis

The data were analyzed using the Graph Pad prism 6 software. All statistical analyses involve use of either one-way or two-way ANOVA (with multiple comparisons) or Student's t-test as required. Statistical significance was accepted at  $p < 0.05$  or lower with a confidence interval of at least 95% or higher depending on the p-value. The values reported in results section (all figures) are mean  $\pm$  standard error mean (SEM) unless otherwise stated.

**Table 3. Primer sequences for qRT-PCR in LLC-PK1 cell samples**

S. No.	Gene	Sequence 5' → 3'
1.	B-actin forward	TCTGGCACACACCTTCTA
	B-actin Reverse	TCTTCTCACGGTTGGCTTTG
2.	BAX Forward	CCCTTTTGCTTCAGGGGATGA
	BAX Reverse	CCGCCACTCGGAAAAAGACT
3.	BID Forward	GGATTCTAAGGTCAGCAACGGT
	BID Reverse	GGATTCTAAGGTCAGCAACGGT
5.	BCL-2 Forward	AGGATAACGGAGGCTGGGATG
	BCL-2 reverse	AGGATAACGGAGGCTGGGATG
6.	MCL-1 Forward	CTAGAAGGCGGCATCAGAAA
	MCL-1 Reverse	GTGGCTGGAGTTGGTTAAGA
7.	EDN-1 Forward	CTGCACTCCGCCTAAAGTATT
	EDN-1 Reverse	GATTTCACGAGGCTAGGATTT

## Chapter 3

### 3 Results

The objective of our study was to evaluate the role of H<sub>2</sub>S supplementation in attenuating the effects of IRI in an *in-vivo* murine model of donation after cardiac death and study the underlying mechanisms in an *in-vitro* model of IRI using porcine proximal tubular epithelial kidney cells. The results from the current study are explained in the next sections.

#### 3.1 Murine Model of Donation after Cardiac Death

The sham-operated rats underwent a midline incision only while the untreated and the treatment group rats received the donor kidneys that had experienced 30 minutes of warm ischemia (clamping) and 18 hours of cold storage in either UW solution alone or UW supplemented with 150µM NaHS respectively. The treatment group donor rats had also received 2mmol/kg D-cysteine I.P. one hour prior to the clamping of the pedicle. This *in-vivo* murine model assesses the effect of H<sub>2</sub>S supplementation on recipient survival, graft function and renal injury by analyzing blood serum, urine and renal graft tissue samples and the results are described below.

##### 3.1.1 Increased survival in treatment group rats

Following renal transplantation, the rats were observed for 30 days. Each group (untreated – cold storage in UW only; treatment – donors received 2mmol/kg D-cysteine I.P. and cold storage in UW +150µM NaHS; and sham – no renal transplant) contained six rats and the sham rats depicted a 100% survival showing efficiency of the surgical technique. Three out of six untreated group rats died on post-operative day 1,2 and 9 respectively. The other three rats from the untreated group survived till the end point (day 30). However, only one treatment rat died on post-operative day 2 while the rest were sacrificed upon reaching the end point. Overall, the treatment group rats showed an increased survival percentage in comparison to the control rats (Figure 6). A significant difference was observed between the survival curves of the three groups ( $p < 0.05$ )

indicating a trend between the groups as per the log rank test for trend used for survival curve analysis.

### 3.1.2 Serum analysis indicates a trend of improved graft function in treatment group

The serum samples collected from the blood of renal transplant recipients (untreated & treatment group) and sham-operated rats were analyzed for various parameters such as serum creatinine, urea and osmolality to compare the renal graft function among the different experimental groups.

The serum creatinine values indicate a trend depicting much faster and consistent recovery in the treatment group (Figure 7). The creatinine values decrease rapidly and approach the sham baseline levels by post-operative day 10 in the treatment group rats. However, for the untreated rats, the creatinine levels show a comparably slow recovery during the initial period following transplantation. One should also keep in mind that half of the untreated group rats that were not doing well were dead by postoperative day 9. As a result, the serum creatinine values for the untreated group rats that did survive the initial vulnerable period were very close to the sham levels.

The serum urea and osmolality levels were also measured and are shown in figures 8 (A) & 8(B), respectively. The serum urea levels followed the same pattern like the serum creatinine (as expected) since both of them mark the ability of the kidneys to remove waste products from the body. The osmolality levels remained consistent among the rats throughout the experimental period indicating normal physiological functioning in these animals.

Although there is a trend showing reduction in delayed graft function among the treatment group rats, no statistically significant differences were observed between the untreated and the treatment group rats in terms of the creatinine, urea and osmolality measured in blood serum on any post – operative day.

### 3.1.3 Urine analysis demonstrates reduced injury in treatment group

The urine collected from the rats on day 3, 5, 10, 20 and 30 was analyzed by measuring the amount of protein and creatinine in the urine. These values were then used to calculate the protein to creatinine ratio, which is an indicator of injury to the renal graft. It was observed that the transplant recipient rats had higher ratio in comparison to the sham-operated rats as expected (Figure 9). Upon statistical analysis using two-way ANOVA with multiple comparisons, statistically significant difference was observed between the untreated and the treatment group rats on post-operative day 5 ( $p < 0.05$ ) with a higher protein to creatinine ratio in the untreated rats in comparison to the treatment group.

The urine osmolality was also measured in these samples and is shown in figure 10. The urine osmolality in the transplant recipients (both untreated and treatment groups) was observed to be significantly lower (\*\* =  $p < 0.01$ , \*\*\* =  $p < 0.001$ , \*\*\*\* =  $p < 0.0001$ ) than the sham group rats using two-way ANOVA with Tukey's multiple comparisons test. Over the time period of 30 days, the osmolality values did seem to increase at a steady rate for both the untreated and the treatment group rats. However, the values did not reach the baseline levels within this time period.

### 3.1.4 ATN scores depict higher histological injury in untreated rats

The scores from the H&E slides scored by the pathologist blinded to the treatment groups are shown in figure 11. The sham group rats did not show any histological injury as indicated by the consistent score of '0' across all five rats. The untreated group rats showed a wider range of injury scores. However, the untreated group rats that were sacrificed on post-operative day 3 showed significantly higher injury score than the sham-operated rats (\* =  $p < 0.05$  using two-way ANOVA with Tukey's multiple comparisons test). In addition, the treatment group rats scored lower on the injury scale and no statistically significant difference was observed between the sham operated and treatment group rats.

### 3.1.5 Comparable amount of apoptosis observed in the untreated and treatment group renal transplant recipients

Using the TUNEL stain, the tissue samples collected from different experimental groups on post-operative day 30 were evaluated for the amount of apoptosis in them. The images of the TUNEL stain slides upon analysis with image-J software did not show any statistically significant differences between the untreated and the treatment group rats (Figure 12).

### 3.1.6 Trends in *mRNA* expression of pro-apoptotic, anti-apoptotic and inflammatory markers in the collected tissue

The results from qRT-PCR depicted some trends in the expression levels of various apoptosis related genes (Figure 13). Although no statistically significant differences were observed, *mRNA* analysis indicated a trend towards reduced expression of pro-apoptotic genes (such as caspase-3, Bax and Bid) and pro-inflammatory gene (TNF- $\alpha$ ) in the treatment group tissue samples (n=4) and increase in the anti-apoptotic marker Bcl-2 in both the untreated and treatment groups.



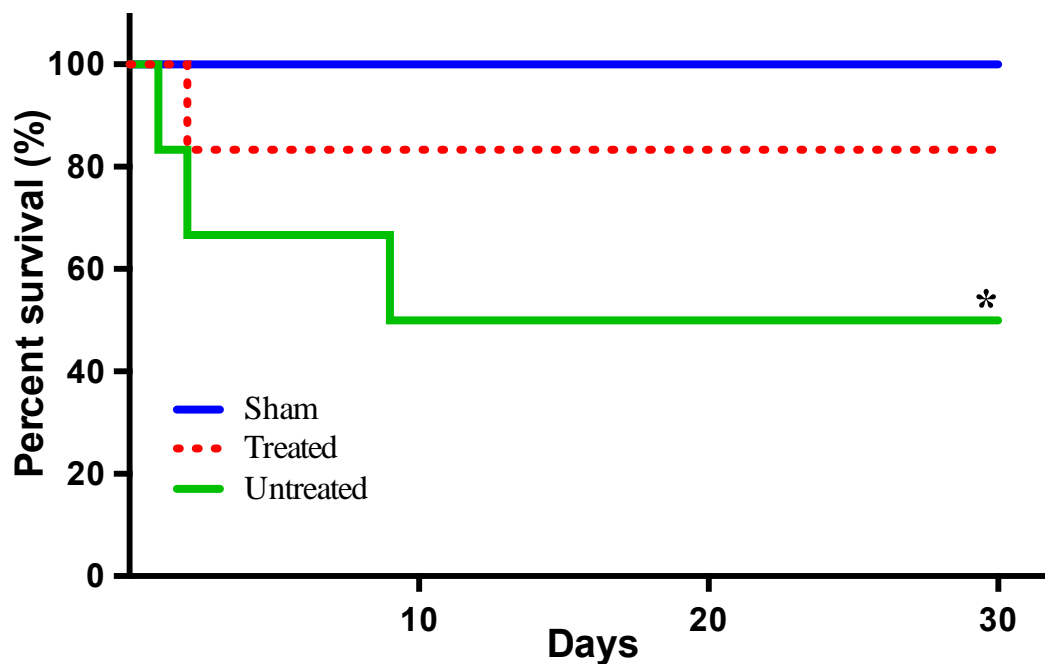


**Figure 6: D-Cysteine and H<sub>2</sub>S supplementation improved survival of renal transplant recipients.**

The graph shows the survival rates of sham-operated rats and renal graft recipients from the treatment and untreated group rats. The donor rats for the treatment group were injected I.P. with D-cysteine (2mmol/kg) and the donor kidneys were perfused and stored in UW solution supplemented with 150 $\mu$ M NaHS. The donor kidneys for the untreated group were perfused and stored in UW solution alone (n = 6 in each group; \* = p < 0.05 as per the log rank test for trend among survival curves).

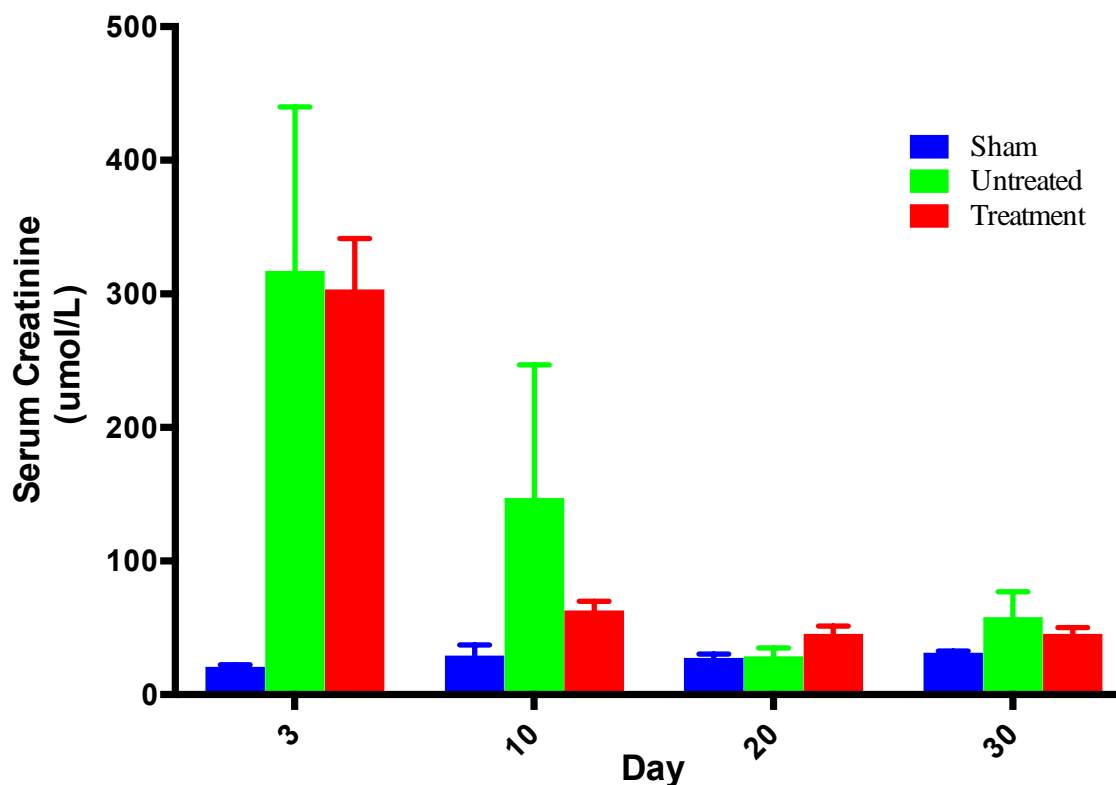


**Figure 7: D-Cysteine and H<sub>2</sub>S supplementation indicates a trend of accelerated recovery in renal graft function following ischemic injury to the renal grafts**

The graph shows the levels of serum creatinine in the sham-operated rats and renal graft recipients from the untreated and treatment groups on post-operative day 3, 10, 20 and 30. The donor rats for the treatment group were injected I.P. with D-cysteine (2mmol/kg) and the donor kidneys were perfused and stored in UW solution supplemented with 150 $\mu$ M NaHS. The donor kidneys for the untreated group were perfused and stored in UW solution alone (Values are Mean  $\pm$  SEM, n = 6 in each group but varies for different days because of variation in survival; differences statistically not significant).

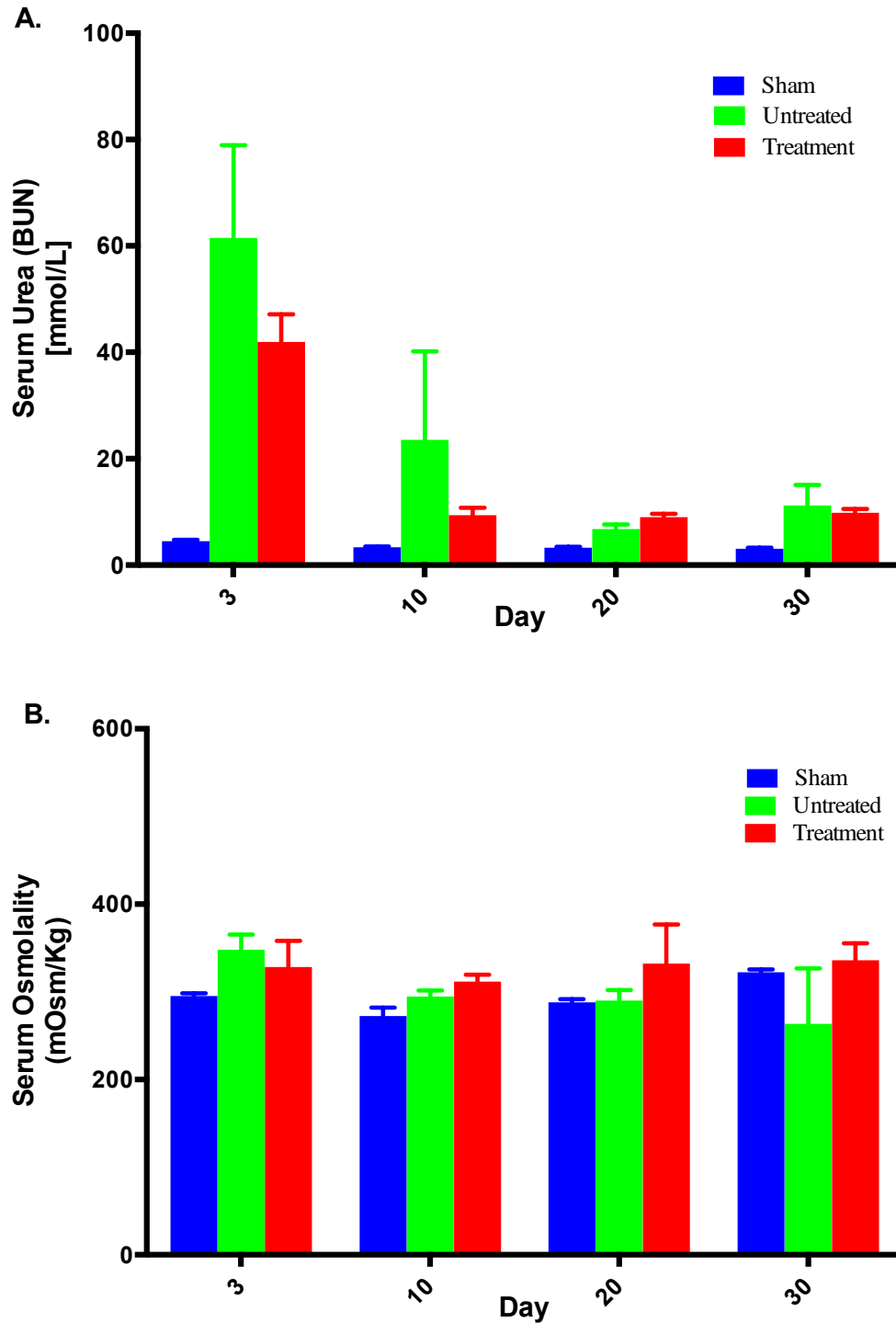


**Figure 8: (A) Serum urea levels depict similar trends as serum creatinine and (B) serum osmolality remains consistent across different experimental groups over the time course of experiment**

The graphs show the levels of serum urea and osmolality in the sham-operated rats and renal graft recipients from the untreated and treatment group on post-operative day 3, 10, 20 and 30. The donor rats for the treatment group were injected I.P. with D-cysteine (2mmol/kg) and the donor kidneys were perfused and stored in UW solution supplemented with 150 $\mu$ M NaHS. The donor kidneys for the untreated group were perfused and stored in UW solution alone. (Values are Mean  $\pm$  SEM, n = 6 total in each group but varies for each day depending on survival as per the experimental group; differences between untreated and treatment groups not significant statistically)

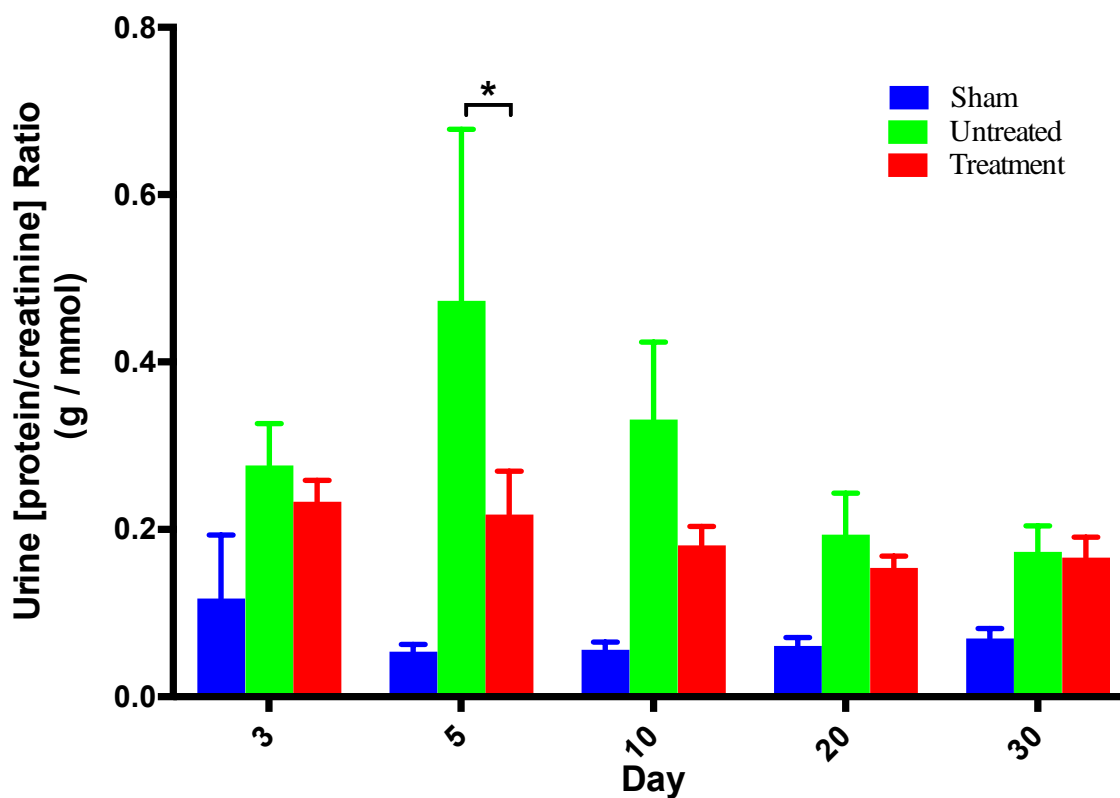


**Figure 9: Urine protein to creatinine ratio indicating inferior kidney function in the untreated group rats in comparison to the treatment group rats**

The graph depicts urine protein to urine creatinine ratio in the sham-operated rats and renal graft recipient rats from the untreated and treatment group on post-operative days 3, 5, 10, 20 and 30. H<sub>2</sub>S supplementation in the treatment rats provided some protection against ischemia reperfusion injury lowering the ratio. A significant difference ( $p < 0.05$ ) in the ratio was observed between the untreated and the treatment group on post-operative day 5. (n=3 in untreated and treatment group; n=5 in sham operated group; \* =  $p < 0.05$  using two-way ANOVA with Tukey's multiple comparisons test)

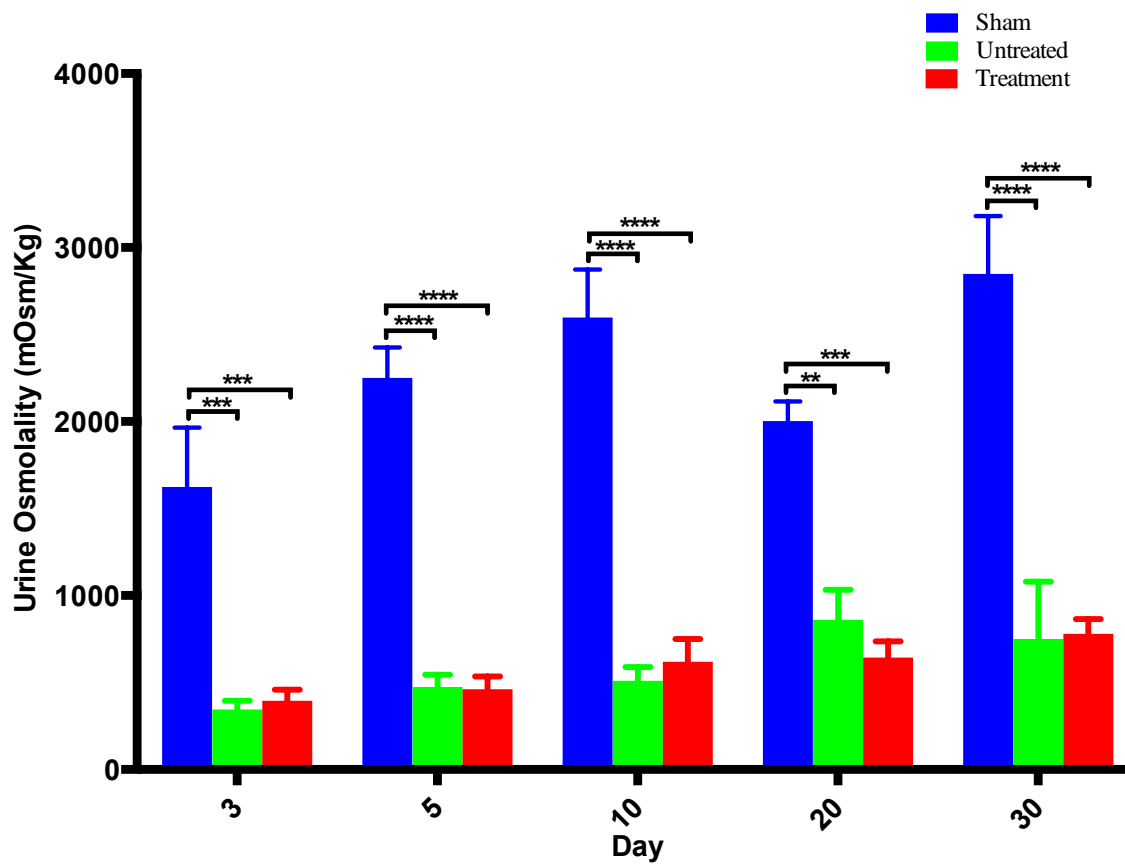


**Figure 10: Decreased urine osmolality in the renal transplant recipients in comparison to the sham-operated rats**

The graphs show urine osmolality in the sham-operated rats and renal graft recipient rats from the untreated and treatment group on post-operative day 3, 5, 10, 20 and 30. The donor rats for the treatment group were injected I.P. with D-cysteine (2mmol/kg) and the donor kidneys were perfused and stored in UW solution supplemented with 150 $\mu$ M NaHS. The donor kidneys for the untreated group were perfused and stored in UW solution alone. The urine osmolality is significantly lower in the renal transplant recipients in comparison to the sham-operated rats. (Values are Mean  $\pm$  SEM, n=3 in untreated and treatment groups; n=5 in sham operated group, \*\* = p<0.01, \*\*\* = p<0.001, \*\*\*\* = p<0.0001 using two-way ANOVA with Tukey's multiple comparisons test)

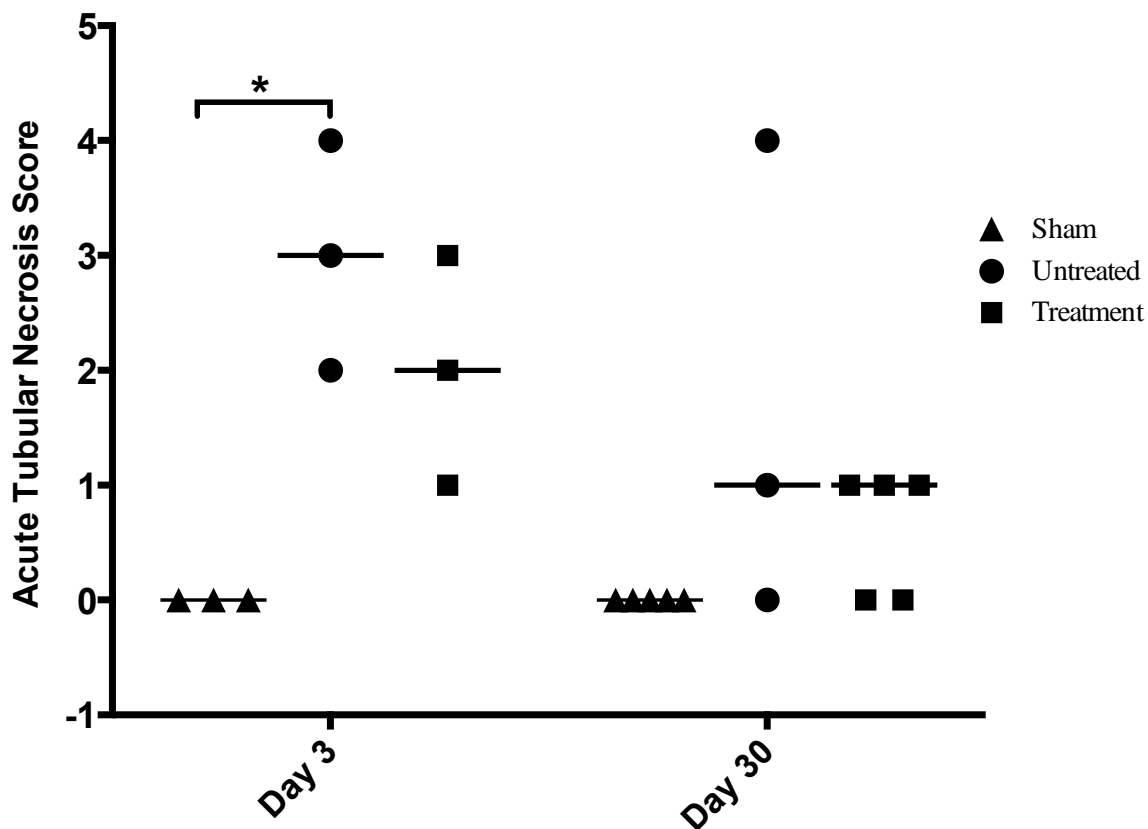


**Figure 11: H<sub>2</sub>S supplementation reduces tissue injury following ischemia reperfusion injury**

The H&E tissue slides scored by the pathologist blinded to the treatment groups showed significant ( $p < 0.05$ ) difference in the acute tubular necrosis scores for the untreated group and the sham operated rats that were sacrificed on post-operative day 3 depicting higher injury in the untreated rats. No significant differences observed between the experimental groups from the tissues collected on post-operative day 30 (\* =  $p < 0.05$  using two-way ANOVA with Tukey's test for multiple comparisons).

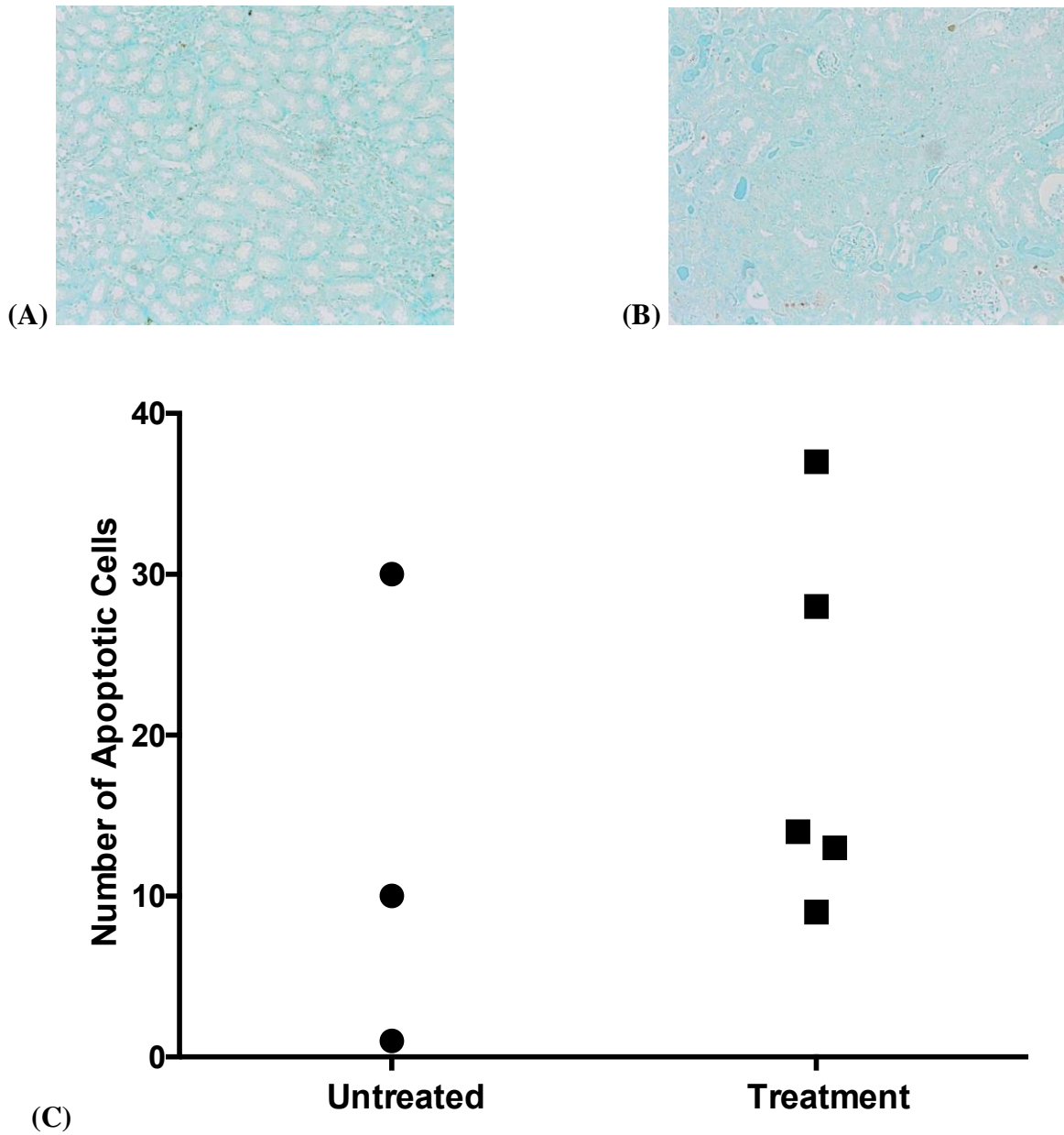


**Figure 12: Number of apoptotic cells in kidney tissue collected from untreated group and treatment group of rats on post operative day 30.**

Image of TUNEL stained tissue sections from untreated group (A) and treatment group (B) at 10X magnification. The scatter plot (C) shows the number of median apoptotic cells in the graft samples from the two groups counted using the Image-J software. The subjects shown above had survived until the end point of post-operative day 30.

(Differences between the untreated and treatment group were not statistically significant)



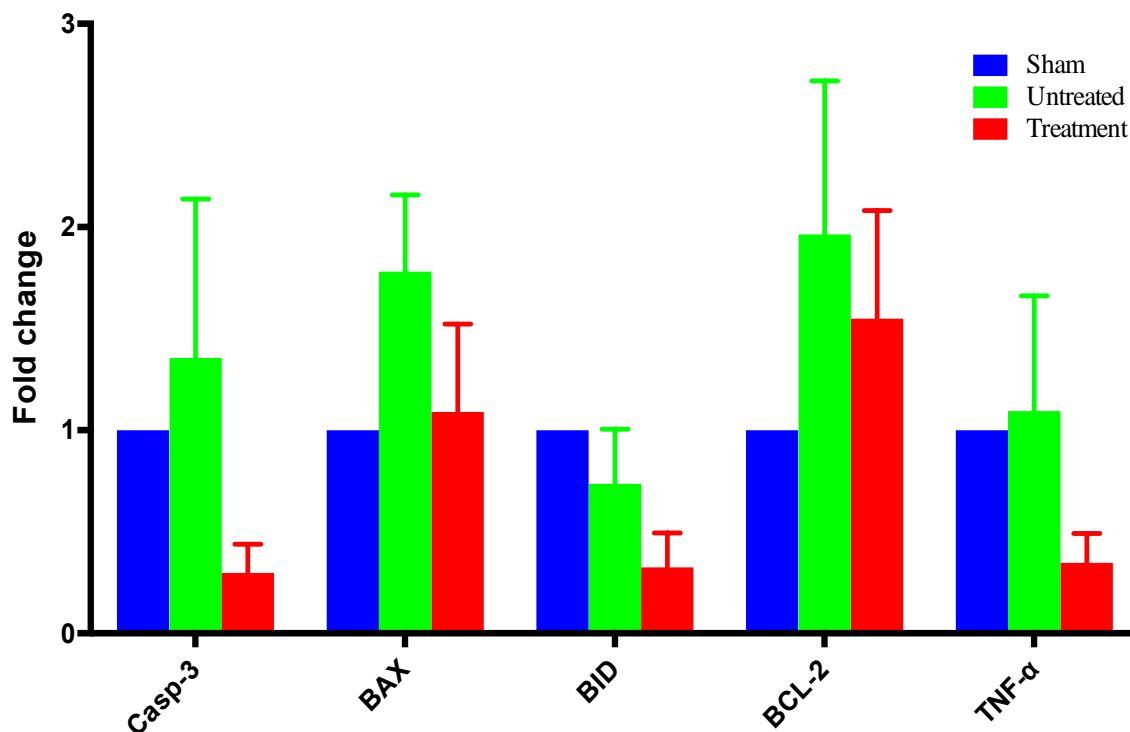


**Figure 13: Differences in the mRNA expression of various apoptosis related genes.**

A trend indicating some down-regulation in the expression of pro-apoptotic and inflammatory markers (Caspase-3, Bid and TNF- $\alpha$ ) was observed in the treatment group while the Bax expression remained at the basal level (as in sham group). The untreated group depicted a trend towards increased expression of Caspase-3 and Bax that feed the apoptosis-signaling cascade. However, no statistically significant differences were observed. (Values are Mean  $\pm$  SEM, n=4 in untreated and treatment group; n=2 in sham-operated group)

## 3.2 *In-vitro* DCD Model

For the *in-vitro* aspect of this project, the porcine proximal tubular epithelial kidney cells were exposed to hypoxic injury in a serum and glucose deprived media and any changes in cell viability (following 24 hour reoxygenation), quantities of ROS and mitochondrial membrane potential were measured using the stains Annexin-V/ 7-AAD, DHR 123 and JC-1 with flow cytometry respectively. These changes were then compared to the cell samples treated with H<sub>2</sub>S donor GYY4137 (50μM). We also looked at the m-RNA expression of apoptosis and injury related marker proteins in our treated and untreated cell samples using qRT-PCR.

Preliminary experiments helped us to choose the time interval for inducing adequate hypoxic injury to LLC-PK1 cells. As shown in figure 14, the increases in cold hypoxic time from 4hours warm + 6hours cold to 4hours warm + 8hours cold does not impact the cell viability and the mean viability of hypoxic samples stays around 65%. In addition, the amount of cell death in 12hours warm + 24 hours cold hypoxic time is comparable to the 12 hours warm alone hypoxia as in both these cases the cell viability goes down by 35%.

### 3.2.1 GYY4137 improved cell viability and decreased necrosis and late apoptosis in LLC-PK1 cells experiencing IRI

The dose response curve for GYY4137 showed the protective effects of H<sub>2</sub>S supplementation on cell viability. The flow analysis scatter plots and bar graph (Figures 15 and 16, respectively) show that the cell viability increases by almost 25% with 50μM and 500μM doses of GYY4137. The percentage of viable cells in untreated (DMEM) samples was 51% while it increased to ~ 74% in cell samples treated with H<sub>2</sub>S donor (DMEM + 50μM/500μM GYY4137). There was a statistically significant difference ( $p < 0.05$ , two way ANOVA with Tukeys test for multiple comparisons) observed between the percentages of viable cells in the untreated (DMEM with no GYY4137) and treated (DMEM + 50 μM GYY4137) cell samples.

Some difference was also observed in the amount of necrotic and late-apoptotic cells while little to no early apoptosis was detected (Figure 17). The percentage of necrotic

cells decreased from 39% in untreated cells to approximately 20% in the cells treated with 50 $\mu$ M and 500 $\mu$ M of GYY4137. A similar decline was observed in the percentage of late apoptotic cells from 9% in untreated samples to 4.5% with the same concentrations of GYY4137. However, the differences between percentages of necrotic and late-apoptotic cells in the treated and untreated samples were not found to be statistically significant and the experiment would need to be repeated in order to discover statistically significant differences.

### 3.2.2 GYY4137 supplementation indicated a trend in reduction of cells with detectable ROS

A trend indicating reduction in the percentage of cells with reactive oxygen molecules is evident in figure 18. Although the differences are not statistically significant and further experiments would be needed to increase the number of samples for finding statistically significant differences, but the current trend in results looks promising as the exogenous supplementation with H<sub>2</sub>S donor helped decrease the amount of cells with detectable ROS. Under normoxic conditions, the percentage of healthy cells (Media) with ROS is around 8%. When these cells are deprived of FBS and glucose, the percentage of cells with ROS goes up to 22% at normal oxygen concentrations. The same glucose/FBS deficient conditions under hypoxia increase the percentage of cells with ROS to 40%. However, addition of 50 $\mu$ M GYY4137 reduces the ROS and thereby lowers the percentage of cells with detectable ROS to 33%.

### 3.2.3 Trend depicting decline in depolarization of the mitochondrial membrane in cells treated with GYY4137

Supplementation with exogenous H<sub>2</sub>S donor also helped decrease the percentage of cells with depolarized mitochondrial membrane as shown by the trend observed in figure 19. The untreated cell samples showed approximately 13% of cells with depolarized mitochondria. Upon treatment with 50 $\mu$ M GYY4137, the percentage of cells with depolarized mitochondrial membrane decreased to about 10% indicating a role played by H<sub>2</sub>S in mitochondrial membrane permeability transition. However, no significant differences were observed between the treated and the untreated cell samples and a higher

number of sample numbers from future experiments would be needed to elucidate statistically significant differences between the two groups.

### 3.2.4 Up-regulation of anti-apoptotic proteins and down-regulation of injury related proteins in treated cells following hypoxia

Analysis of mRNA samples showed significant differences in the expression of various apoptosis and injury related markers in the cell samples (Figure 20). A significant increase in the expression of anti-apoptotic markers Mcl-1 ( $p < 0.001$ ) and Bcl-2 ( $p < 0.01$ ) was observed in cells treated with 50 $\mu$ M GYY4137 in comparison to untreated hypoxic cells. There was also a significant reduction in the expression of injury marker EDN-1 in the treated samples ( $p < 0.01$ ) in comparison to the untreated hypoxia exposed cell samples. However, a trend of decreased expression of pro-apoptotic molecules (not statistically significant) was observed across all samples (whether treated or untreated) consistently.

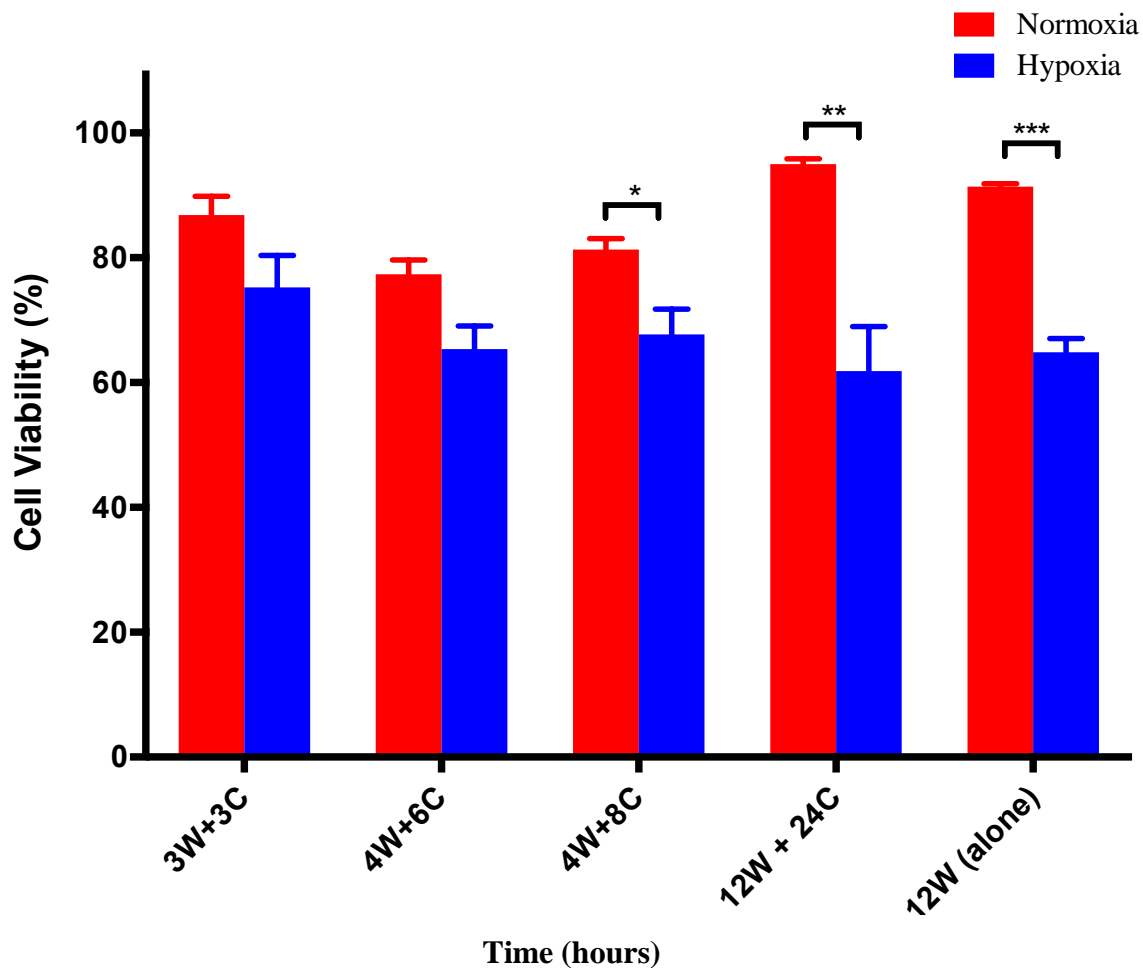


**Figure 14: Different combinations of warm and cold hypoxic times and resulting impact on cell viability.**

Preliminary experiments indicating little to no change in hypoxic sample's cell viability upon incremental increases in just the cold hypoxic time. Statistically significant negative impact observed on cell viability in 4hours warm + 8 hours cold ( $p < 0.05$ ), 12hours warm + 24 hours cold ( $p < 0.01$ ) and 12 hours warm alone ( $p < 0.001$ ) conditions in comparison to normoxic-healthy cells. (W = warm hypoxic hours, C = cold hypoxic hours; Values are Mean  $\pm$  SEM,  $n=4$  in each group, \* =  $p < 0.05$ , \*\* =  $p < 0.01$ , \*\*\* =  $p < 0.001$  using Student's t-test)

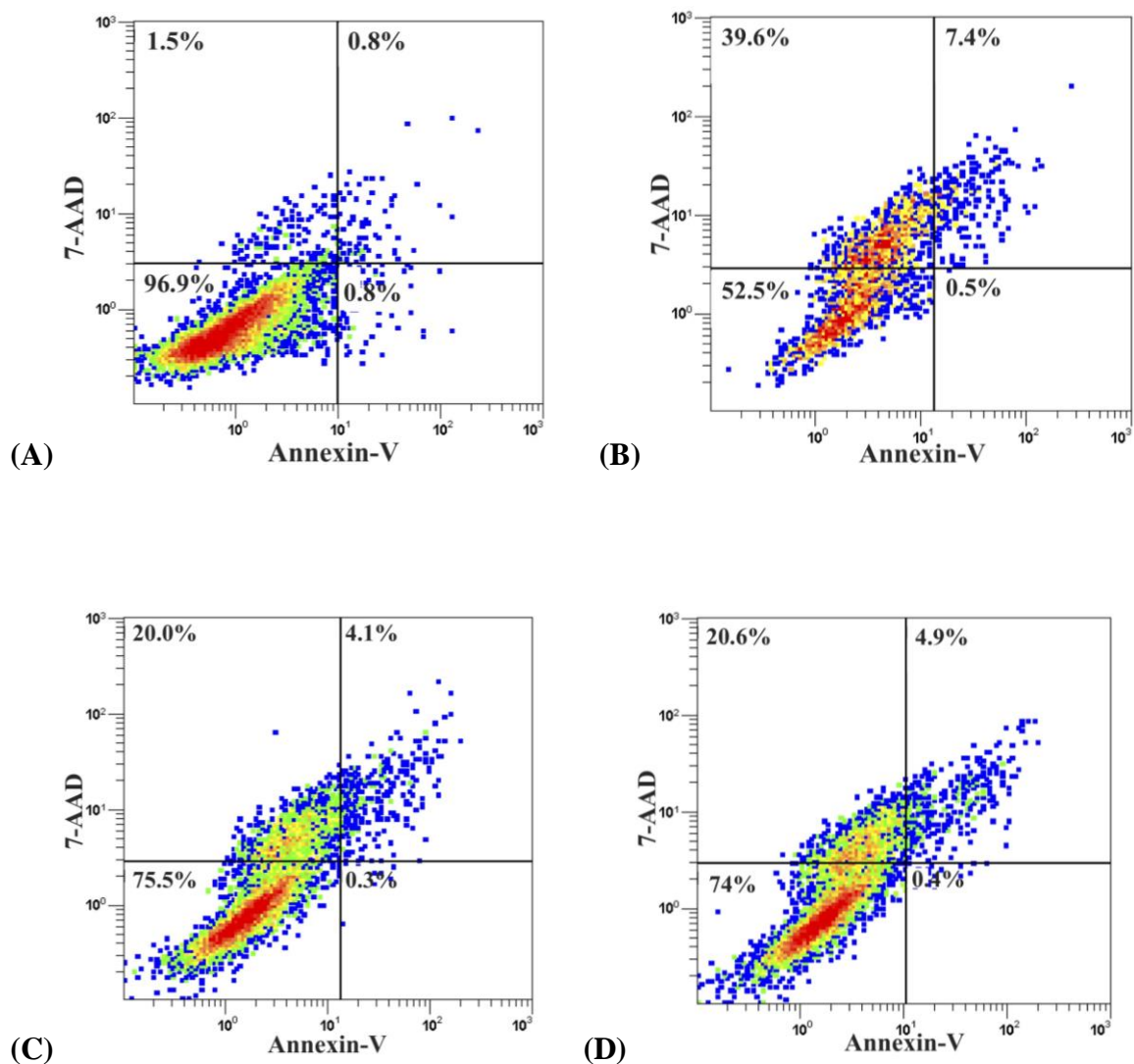


**Figure 15: Flow analysis scatter plots obtained from Annexin-V and 7-AAD staining**

The plots above represent the healthy cells under normoxic conditions in incubator (A), the hypoxic untreated samples (B) and cell samples supplemented with 50 $\mu$ M and 500 $\mu$ M GYY4137 respectively (C & D). The x-axis is representative of Annexin-V stain and y-axis represents 7-AAD stain. The upper left quadrant marks the necrotic cells, lower left quadrant has the healthy cells, the upper right quadrant shows the late apoptotic/necroptotic cells while the lower right quadrant has the early apoptotic cells.

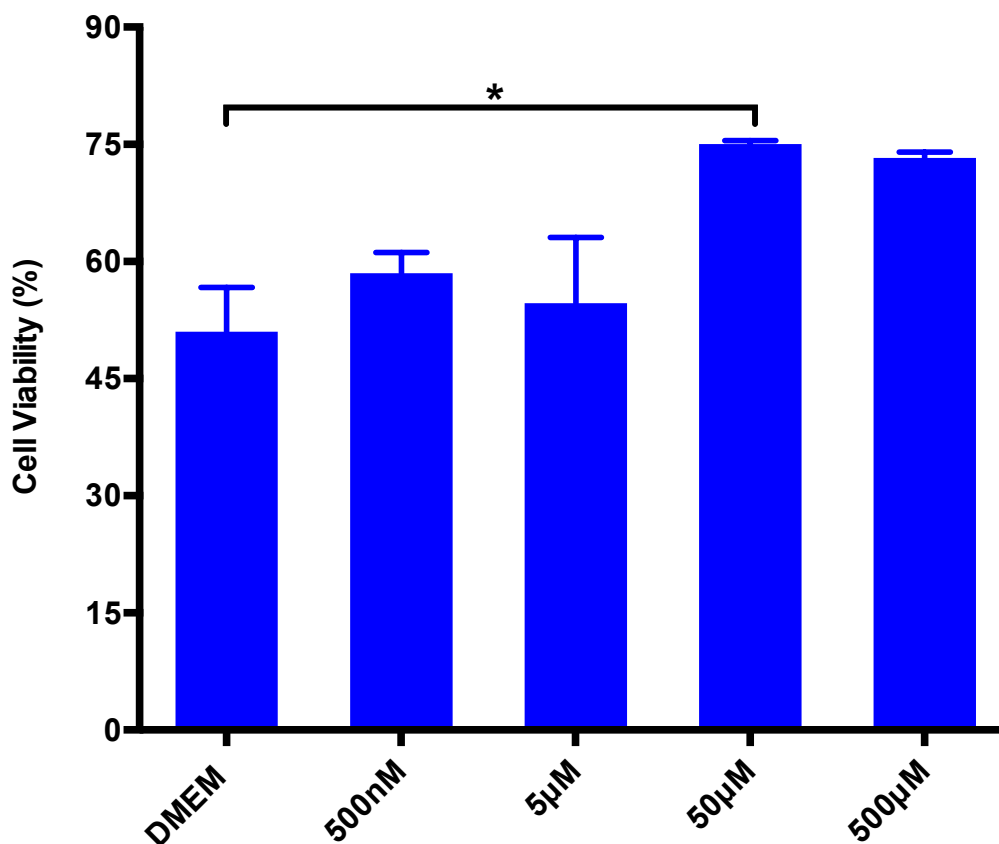


**Figure 16: Increased percentage of viable cells upon supplementation with GYY4137.**

Cell samples exposed to 12 hours hypoxia and 24 hours reoxygenation (at 37°C) were analyzed for cell viability using Annexin-V and 7-AAD stains with flow cytometer. Adequate concentration of GYY4137 (50µM) helps mitigate effects of hypoxia-reoxygenation injury in LLC-PK1 cells. The cell viability is significantly improved in the treatment group ( $p < 0.05$ ) in comparison to the untreated group. (Values are Mean  $\pm$  SEM,  $n=3$  in each group, \* =  $p < 0.05$  using two-way ANOVA with Tukey's test for multiple comparisons)

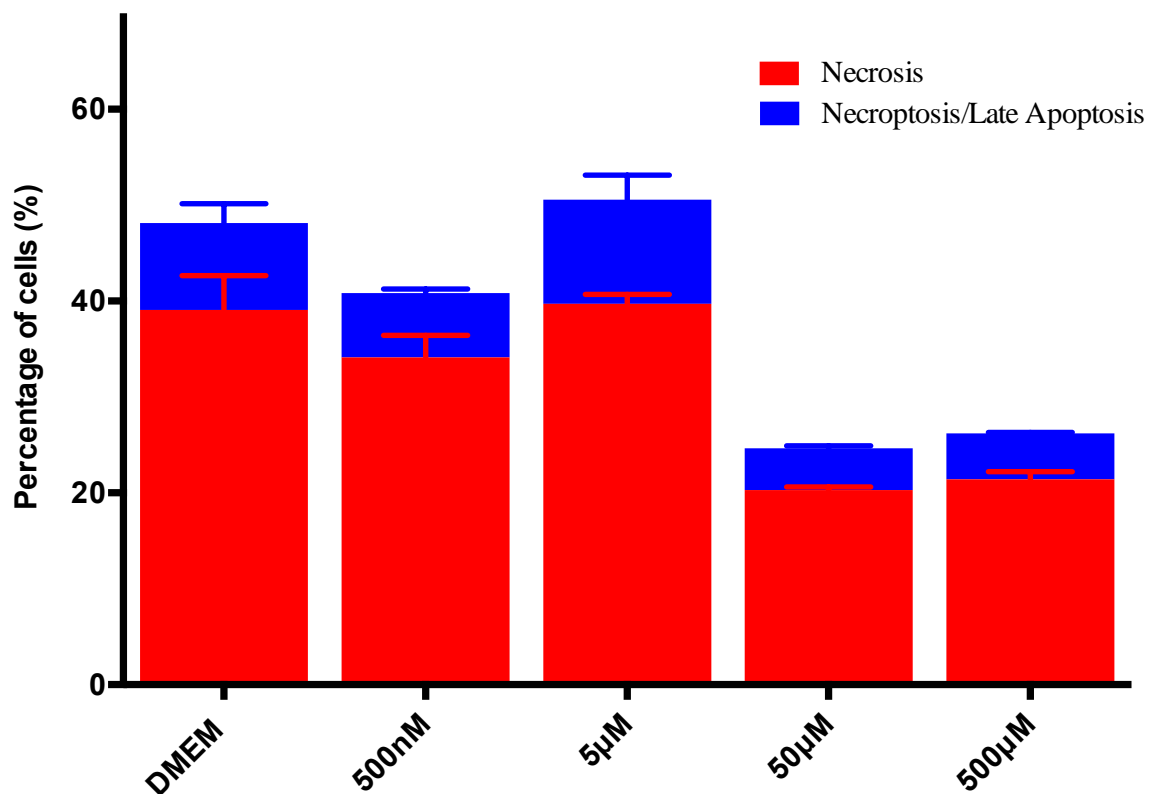


**Figure 17: Trend depicting decrease in percentages of necrotic and late apoptotic cells after supplementation with H<sub>2</sub>S donor.**

The percentage of necrotic and late apoptotic cells is reduced to half the amount of that observed in untreated samples after experiencing 12 hours of hypoxia at 37°C followed by 24 hours of reoxygenation. The cells were analyzed using the Annexin-V and 7-AAD stains using flow cytometer. (Red = percentage of necrotic cells, Blue = percentage of late apoptotic/necroptotic cells; Values are Mean ± SEM, n=3 in each group, differences are not statistically significant)



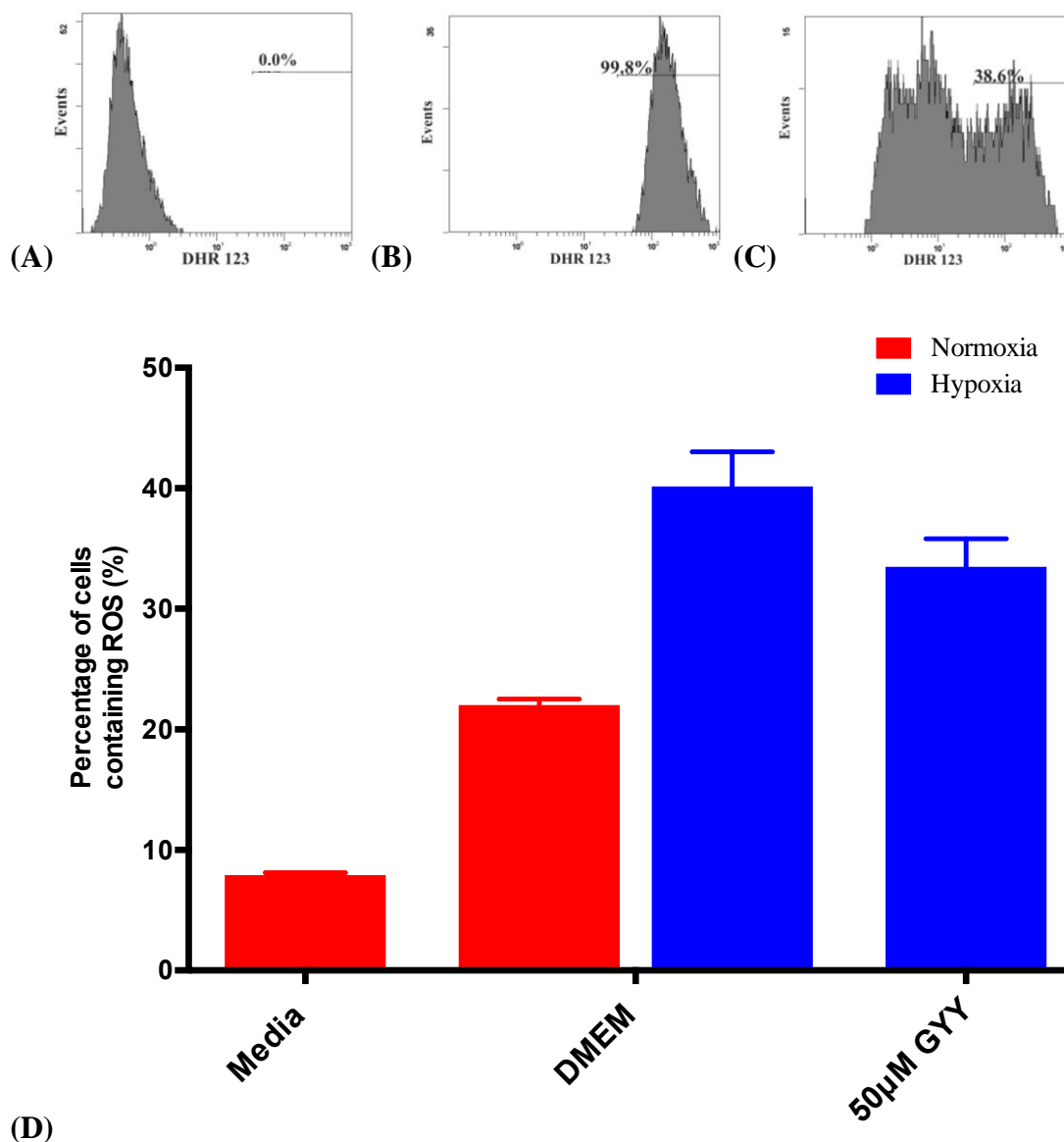


**Figure 18: Trend indicating reduction in percentage of cells with reactive oxygen species upon  $H_2S$  supplementation.**

Following 12 hours of hypoxia, treated and untreated cell samples were stained with DHR123 and analyzed with flow cytometer. The histograms from flow analysis show the unstained-negative untreated (A), positive control - cells treated with 3%  $H_2O_2$  in PBS for 10 minutes (B), and a sample of untreated cells after hypoxia (C). The bar graph in (D) shows reduced percentage of cells with ROS upon supplementation with 50µM of GYY4137 during hypoxic phase. (Mean  $\pm$  SEM, n=4 in each group, differences statistically not significant)

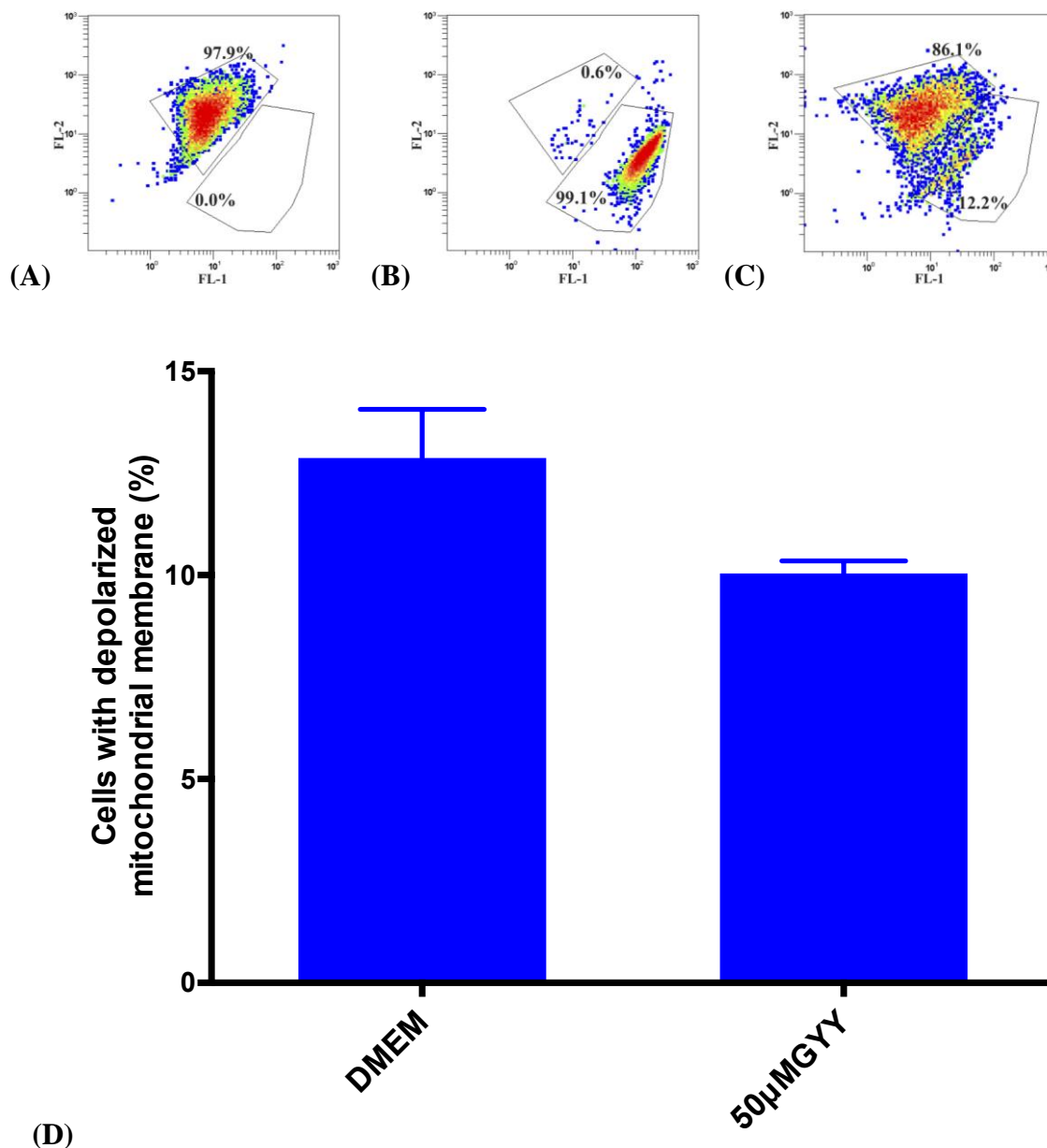


**Figure 19: Trend depicting decreased percentage of cells with depolarized mitochondrial membrane in treated sample.**

The scatter plots from flow analysis show healthy cells (A), heat killed positive control (B) and untreated (DMEM only) cell sample (C) stained with JC-1 molecule following 12 hours of hypoxia at 37°C. The bar graph (D) shows a trend of decrease in percentage of cells with depolarized mitochondrial membrane upon addition of 50µM GYY4137 during hypoxic conditions. (Values are Mean  $\pm$  SEM, n=4 in each group, differences statistically not significant)

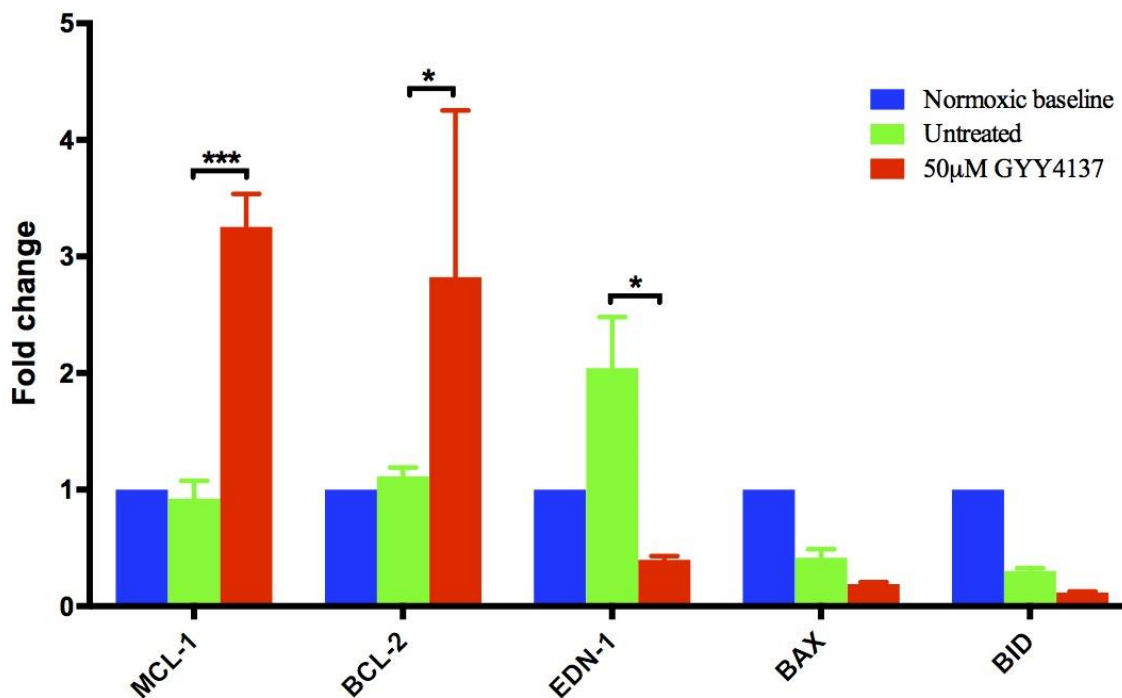


**Figure 20: Up-regulation of anti-apoptotic proteins while down regulation of injury markers observed with H<sub>2</sub>S supplementation.**

Increase in mRNA expression of Bcl-2 and Mcl-1 (anti-apoptotic proteins) along with decreased expression of injury marker EDN-1 observed in cells treated with 50µM GYY4137. The pro-apoptotic markers were down regulated in all samples irrespective of H<sub>2</sub>S supplementation. (Values are mean ± SEM and n=4 in each group; two-way ANOVA with Tukey's test for multiple comparisons used; \* = p<0.05, \*\*\* = p<0.001)

## Chapter 4

### 4 Discussion

Renal transplantation is considered to be the most effective renal replacement therapy in ESRD patients. Due to the disparity between the organ demand and supply, the use of marginal donors (such as DCD donors) has become acceptable. However, the DCD grafts experience prolonged IRI and are more susceptible to failure and delayed graft function. Thus, finding ways to mitigate IRI in these grafts has become the prime focus of the transplant community.

Our lab has previously shown the protective effects of supplementation with exogenous H<sub>2</sub>S on graft function after either prolonged warm ischemia or cold storage.<sup>90,112</sup> However, the murine model of renal transplantation used in this study is the first of its kind to use a combination of both warm ischemia and cold storage and mimics the clinical model of a DCD transplant. The DCD murine model used in this study showed improved graft function and survival rate in the recipients with concurrent exogenous (NaHS) and endogenous (D-cysteine/3MST pathway) H<sub>2</sub>S supplementation. This is in accordance with other renal IRI studies performed in mice or rats showing protective effects of either exogenous H<sub>2</sub>S addition involving 30 minutes to 1 hour of pedicle clamping (warm ischemia)<sup>84,90,112</sup> or showing how endogenous H<sub>2</sub>S also helps mitigate effects of IRI in renal models.<sup>113</sup> L-cysteine is a widely used substrate for H<sub>2</sub>S production endogenously through the CBS and CSE enzymatic pathways. It generally overshadows the role played by D-cysteine in H<sub>2</sub>S production internally. However, a recent study by Shibuya and Kimura (2013) showed that D-cysteine diminishes impact of IRI more effectively than L-cysteine because of its 80-fold greater H<sub>2</sub>S producing activity in the kidney.<sup>105</sup> This is the reason why I chose to incorporate a combination of D-cysteine and exogenous H<sub>2</sub>S supplementation in our experimental study.

H<sub>2</sub>S supplementation in this model of prolonged warm ischemia and cold storage followed by subsequent renal transplantation led to increased survival rate, faster recovery of graft function and less renal injury in treatment group rats. By post-operative

day 10, the treatment group's serum creatinine was almost equivalent to the baseline sham levels while it took almost 20 days for the untreated group to reach the baseline levels. This indicates prevention of delayed graft function in the recipients that could help eliminate the need for dialysis after the first week of transplantation. The urine osmolality, on the other hand, was lower for both the untreated and treatment groups in comparison to the sham group rats. Decreased urine osmolality is a marker of either impaired renal function or diuresis in the transplant recipients as another study has reported diuresis in the transplant recipients in an IRI model.<sup>112</sup> However, further analysis such as the glomerular filtration rate along with the concentration of various ions (like sodium and potassium) in urine and blood serum can help elucidate the actual cause of decrease in urine osmolality for the subjects in our study.

One of the ways in which our study is different from others is the length of the experimental period (30 days). This helped us to look at the long-term effects rather than limiting it to earlier time points of 2-weeks or less. Tissue analysis indicated comparable amounts of acute tubular necrosis and apoptosis among the untreated and treatment group rats. Other studies have observed comparable increases in apoptosis and necrosis in non-transplantation *in-vivo* IRI models involving clamping induced warm ischemia in renal tissue<sup>84</sup> and myocardium.<sup>89,104</sup>

For studying the IRI mechanism at a cellular level, the proximal tubular epithelial kidney cells are considered to be the prime choice. The reason for this preference stems from the fact that maximum I/R injury is observed in the epithelial cells of the proximal tubular region in the nephrons depicted by the loss of apical brush border.<sup>114</sup> One can argue that the *in-vitro* experiments are limited in their ability to exactly replicate the internal physiologic environment as experienced by the cells during *in-vivo* IRI models, but they are still considered to be the best way to tease apart the cellular signaling pathways and mechanisms.

*In-vitro* studies have shown that the hypoxia-reoxygenation model mimics a similar kind of injury as sustained by the kidney during *in-vivo* IRI. However, different studies vary in the methods of inducing hypoxia that can involve the use of chemicals (mitochondrial

electron transport chain inhibitors like rotenone, antimycin A and sodium azide), enzymatic pathway (Glucose oxidase-GOX and Catalase-CAT; generally called the GOX/CAT system) or a hypoxia chamber (varying concentrations of oxygen - 0.5% to 1% and carbon dioxide – 5% - 20%).<sup>114-117</sup> For this study, I used a precisely regulated hypoxia chamber (as described in methods) to induce the hypoxic injury at 1% oxygen for 12 hours and maintaining 37°C temperature followed by 20-24 hours of reoxygenation. The time interval for hypoxia was based on a number of optimization experiments with varying time periods as was described in the results section.

Our *in-vitro* hypoxia-reoxygenation experiments corroborated results obtained in our *in-vivo* DCD murine model. The addition of slow releasing H<sub>2</sub>S donor (GYY4137) was able to rescue the cells from *in-vitro* hypoxia-reoxygenation injury as observed by increased percentage of cell viability and decreased percentage of necrosis and late apoptosis in the specific cell samples containing 50µM GYY4137. Similar protective effects of H<sub>2</sub>S supplementation have been observed in other *in-vitro* studies involving the use of NaHS in either chemically induced hypoxia in human skin keratinocytes or hypoxia induced by chamber in human umbilical vein endothelial cells (HUVECs).<sup>118,119</sup> However, these effects have not been tested in kidney cell lines. A study performed many years ago by Wiegele *et al.* (1998) showed that the mechanisms of cell death happening from ATP depletion involved apoptosis and necrosis. In their study, apoptosis was observed only at early stages and only in a small proportion of cells while the necrotic pathway was the major culprit of cell death especially with longer periods (more than 8 hours) of ATP depletion.<sup>117</sup> A similar trend was observed in our *in-vitro* model whereby the prolonged hypoxic conditions triggered the necrotic cell death.

One challenge was to assess early apoptotic cells *in-vitro*. Studies by Bursch *et al.* in 1990 noted that the time span from initiation to completion of apoptosis could be as short as 2-3 hours.<sup>120,121</sup> Hence, by the time the cells are analyzed, there is a high possibility that the early apoptotic cells become late apoptotic or necroptotic. This explains why early apoptosis might have gone un-detected in our *in-vitro* experiments. On the other hand, contradictory findings have been reported in literature in regards to apoptosis versus necrosis contribution to cell death. One study of cutaneous tissue transplantation has

reported increased apoptosis along with necrosis following IRI<sup>119</sup> and the same was observed in our *in-vivo* model as well. However, it must be noted that IRI based *in-vitro* studies of hypoxia-reoxygenation look at longer time points and generally report the late apoptotic cells.

Although there might be differences in the extent of apoptosis and necrosis observed after IRI, the cellular pathways and pathophysiology associated with the two processes is very similar ultimately resulting in cell death. Both the processes stem from increased ROS and mitochondrial membrane depolarization. Our *in-vitro* experiments showed a trend of reduction in the percentage of cells with ROS in cell samples supplemented with H<sub>2</sub>S donor. Despite the fact that the amount of ROS present in the treatment group was not significantly lower than the untreated group, even a slight decline in ROS could potentially prove beneficial for rescuing the cells considering the negative impact ROS has on mitochondria and the cell as a whole. The use of stain DHR 123 for detection of ROS has been well established in literature as it has been previously used for studying oxidative burst in human granulocytes.<sup>122</sup> One drawback for using this stain is its higher sensitivity to H<sub>2</sub>O<sub>2</sub> in comparison to other reactive molecules resulting from IRI such as superoxides and per-oxy-nitrites. Superoxide constitutes majority of the ROS and is formed mainly in the mitochondria where it then reacts with the mitochondrial enzymes to form H<sub>2</sub>O<sub>2</sub>.<sup>123,124</sup>

The mitochondrial apoptotic pathway is one of the major contributors of apoptotic cell death while the other pathway that feeds apoptosis is the signaling by death receptors. The mitochondrial pathway involves the crucial process of mitochondrial outer membrane permeabilization (MOMP).<sup>102,125</sup> One of the ways in which this is achieved is the formation of the permeability transition pore that leads to a change in the mitochondrial membrane potential due to equilibration of ions across the membrane.<sup>126</sup> This eventually leads to swelling of the mitochondria followed by breaking of the outer membrane producing MOMP.<sup>125</sup> In this study, it was observed that the addition of H<sub>2</sub>S donor in adequate amounts resulted in a decline in percentage of cells with depolarized mitochondrial membrane. This indicates that H<sub>2</sub>S hinders the MOMP by preventing the permeability transition pore from causing the leakage of ions and thereby impeding

depolarization of the mitochondrial membrane. However, this study did not explore if H<sub>2</sub>S actually blocks these pores or inhibits the formation of these pores to prevent depolarization.

The second mechanism for MOMP is mediated by the members of the Bcl-2 protein family. It is widely accepted that certain members of the Bcl-2 family are pro-apoptotic (such as Bax, Bak or Bid) while others act as anti-apoptotic molecules (such as Bcl-2, Mcl-1).<sup>46</sup> The Bcl-2 is the prototype member of this family of proteins and all members contain at least one Bcl-2 homology (BH) region. The mRNA expression of these proteins was assessed via qRT-PCR in both the *in-vivo* and *in-vitro* samples. The *in-vivo* samples showed up regulation of apoptotic proteins such as caspase-3 and Bax in the rats from untreated group. Still other pro-apoptotic (Bid) and inflammatory (TNF- $\alpha$ ) molecules showed similar expression as the baseline sham levels. However, the same apoptotic and inflammatory markers were highly down regulated in the treatment group rats except the Bax protein that was being expressed at baseline levels. On the contrary, the pro-apoptotic proteins depicted a trend of down regulation in both the treated as well as untreated cell samples in the *in-vitro* experiments.

Previous studies have shown a link between Bax expression and induction of apoptosis in cells.<sup>127</sup> Bax and Bid are generally present in the cytosol of the cells. Upon initiation of apoptotic signaling pathways, these molecules help in inducing MOMP and the eventual leakage of cytochrome c and other proteins from the mitochondria that result in apoptosis in the cells.<sup>125,128</sup> However, these molecules are not solely responsible for MMPT as a study by De Marchi *et al.* showed that blocking the pro-apoptotic proteins like the Bax/Bid did not completely inhibit the depolarization of the mitochondrial membrane in the cells.<sup>129</sup> They also showed that other mechanisms like high intracellular concentrations of Ca<sup>+2</sup> could still result in MMPT in absence of Bax/Bid. This explains some differences observed in the expression of pro-apoptotic proteins in the *in-vivo* and *in-vitro* models in our study since the Bax was not upregulated in the LLC-PK1 cells undergoing IRI but still apoptosis was observed in these samples.



One anomaly observed in our *in-vivo* experiments was the up regulation of Bcl-2 in both the untreated and the treatment group rats while our *in-vitro* hypoxia-reoxygenation model showed a significant up regulation in the mRNA expression of anti apoptotic proteins Mcl-1 and Bcl-2 only in the cell samples treated with 50 $\mu$ M GYY4137. There was also a significant decrease detected in the expression of injury marker EDN-1 in the same cell samples that were supplemented with H<sub>2</sub>S donor in comparison to the untreated cell samples. One of the reasons that can help explain this conflict between the results from *in-vivo* and *in-vitro* experiments is the time point at which the data were collected. The graft tissues used for qRT-PCR were collected from the renal transplant recipient rats on post-operative day 3 while the mRNA was collected from the LLC-PK1 cells right after experiencing 12 hours of warm hypoxia followed by 15 minutes of reoxygenation.

## Chapter 5

### 5 Future Directions

Our *in-vivo* murine model, although first of its kind to mimic DCD renal transplantation, studies the combined effect of increasing endogenous H<sub>2</sub>S production prior to ischemia along with exogenous H<sub>2</sub>S supplementation during the cold storage phase of the graft. It would be interesting to observe the two conditions separately and to see if the effects of endogenous and exogenous H<sub>2</sub>S are synergic in nature. Further, the verification of various apoptotic or anti-apoptotic proteins in the tissue samples using western blots might help solidify the results obtained through mRNA analysis.

The results from *in-vitro* experiments did not show a large number of early apoptotic cells after hypoxic injury and 24 hours of reoxygenation. However, the ROS and mitochondrial membrane potential analysis that was performed after smaller periods or no reoxygenation showed some differences between the untreated and treatment group samples. It would be intriguing to measure percentage of apoptotic cells following smaller periods of reoxygenation after the hypoxic injury. Maybe, a time-course experiment could help shed some light on this phenomenon. In addition, to better understand the mechanism of H<sub>2</sub>S action in mitochondrial apoptotic pathway, the leakage of mitochondrial cytochrome c into the cytoplasm could be studied. This can be done by separating the mitochondrial and cytosolic contents and then measuring the concentration of cytochrome c in each separately. An increase in the ratio of the mitochondrial to cytoplasmic cytochrome c in treated samples would indicate a definitive role of H<sub>2</sub>S in preventing MOMP.

Our study focused on only one H<sub>2</sub>S releasing donor molecule (GYY4137). However, it would be fascinating to see the effect of other H<sub>2</sub>S donor molecules that release H<sub>2</sub>S in a targeted way or stimulate endogenous production of H<sub>2</sub>S. One such recently discovered molecule is AP39 that is a targeted mitochondrial H<sub>2</sub>S donor. Since one of the major apoptotic pathways and cell death mechanism involves the mitochondria, this molecule might prove to be the ideal candidate for future studies.

## Chapter 6

### 6 Conclusion and Significance

Our study is the first ever study looking at the use of H<sub>2</sub>S in a clinically relevant murine model of DCD renal transplantation. Other studies that demonstrate the protective effects of H<sub>2</sub>S against IRI do not involve the transplantation of the organ experiencing IRI into the recipient. The few exceptional studies that do involve renal transplantation fail to investigate the combined effect of warm ischemia and prolonged cold storage. In our study, H<sub>2</sub>S supplementation resulted in increased survival and improved renal graft function along with a significant decrease in histological injury among the treatment group rats. The *in-vitro* model also recapitulated the protective role of slow releasing H<sub>2</sub>S donor molecule (GYY4137) on the proximal tubular porcine kidney epithelial cells (LLC-PK1) as shown by the reduction in depolarization of the mitochondrial membrane, the ROS and the increased cell viability in treated cell samples. It also exemplifies an important role played by the mitochondria in cell death caused by the hypoxia-reoxygenation injury as depicted by up regulation of the mitochondrial associated anti-apoptotic marker Bcl-2, Mcl-1 and decreased expression of pro-apoptosis related genes such as Bax and Bid.

The results from this study illustrate the clinical significance of H<sub>2</sub>S mediated protective pathways in IRI and the future of DCD transplants. Considering the short half-life of H<sub>2</sub>S and its depletion by the time of transplantation in the recipients, it should be feasible to make minimal changes to the current clinical protocol and adopt the use of H<sub>2</sub>S into clinical practice. This transition would not only help to reduce the extent of IRI and delayed graft function experienced by the DCD organs but may also help increase the pool of donors that are deemed suitable for renal transplantation.

## Bibliography

1. St Peter WL. Introduction: chronic kidney disease: a burgeoning health epidemic. *J Manag Care Pharm.* 2007;13(9 Suppl D):S2-S5.
2. About Chronic Kidney Disease - The National Kidney Foundation. <https://www.kidney.org/kidneydisease/aboutckd>. Accessed June 17, 2015.
3. Weiner DE. Causes and consequences of chronic kidney disease: implications for managed health care. *J Manag Care Pharm.* 2007;13(3 Suppl):S1-S9.
4. Usrds. 2013 USRDS annual data report. 2013:464.
5. Information CI for H. Canadian Organ Replacement Register Annual Report : Treatment of End-Stage Organ Failure in Canada , 2003 to 2012. 2014.
6. Murtagh FEM, Addington-Hall J, Higginson IJ. The prevalence of symptoms in end-stage renal disease: a systematic review. *Adv Chronic Kidney Dis.* 2007;14(1):82-99. doi:10.1053/j.ackd.2006.10.001.
7. Baigent C, Burbury K, Wheeler D. Premature cardiovascular disease in chronic renal failure. *Lancet.* 2000;356(9224):147-152. doi:10.1016/S0140-6736(00)02456-9.
8. Torpy JM, Lynn C, Golub RM. Kidney Transplantation. *JAMA J Am Med Assoc.* 2011;305(6):634-634. doi:10.1001/jama.305.6.634.
9. Dialysis | Definition of dialysis by Merriam-Webster. <http://www.merriam-webster.com/dictionary/dialysis>. Accessed June 18, 2015.
10. Himmelfarb J, Ikizler TA. Hemodialysis. *N Engl J Med.* 2010;363(19):1833-1845. doi:10.1056/NEJMra0902710.
11. Hemodialysis: Treatment for Kidney Failure. <http://www.medicinenet.com/hemodialysis/article.htm>. Accessed June 18, 2015.

12. Daugirdas JT, Blake PG, Ing TS. Handbook of Dialysis. In: *Handbook of Dialysis*. Vol 4th ed. Wolters Kluwer; 2006:323-336. [http://www.amazon.ca/Handbook-Dialysis-John-T-Daugirdas/dp/0781752531/ref=sr\\_1\\_1?s=books&ie=UTF8&qid=1434598272&sr=1-1&keywords=9780781752534](http://www.amazon.ca/Handbook-Dialysis-John-T-Daugirdas/dp/0781752531/ref=sr_1_1?s=books&ie=UTF8&qid=1434598272&sr=1-1&keywords=9780781752534).
13. Alloatti S, Manes M, Paternoster G, Gaiter AM, Molino A, Rosati C. Peritoneal dialysis compared with hemodialysis in the treatment of end-stage renal disease. *J Nephrol*. 13(5):331-342.
14. Wu AW, Fink NE, Marsh-Manzi JVR, et al. Changes in quality of life during hemodialysis and peritoneal dialysis treatment: generic and disease specific measures. *J Am Soc Nephrol*. 2004;15(3):743-753. doi:10.1097/01.ASN.0000113315.81448.CA.
15. Purnell TS, Auguste P, Crews DC, et al. Comparison of life participation activities among adults treated by hemodialysis, peritoneal dialysis, and kidney transplantation: A systematic review. *Am J Kidney Dis*. 2013;62(5):953-973. doi:10.1053/j.ajkd.2013.03.022.
16. Nakamura-Taira N, Muranaka Y, Miwa M, Kin S, Hirai K. Views of Japanese patients on the advantages and disadvantages of hemodialysis and peritoneal dialysis. *Int Urol Nephrol*. 2013;45(4):1145-1158. doi:10.1007/s11255-012-0322-x.
17. Coping With The Top Five Side Effects of Dialysis - The National Kidney Foundation. <https://www.kidney.org/news/ekidney/january12/top5>. Accessed June 24, 2015.
18. Kidney Transplant - The National Kidney Foundation. <https://www.kidney.org/atoz/content/kidneytransnewlease>. Accessed June 24, 2015.

19. Suthanthiran M, Strom TB. Renal transplantation. *N Engl J Med*. 1994;331(6):365-376. doi:10.1056/NEJM199408113310606.
20. Mathur AK, Ashby VB, Sands RL WR. Geographic variation in end-stage renal disease incidence and access to deceased donor kidney transplantation. *Am J Transpl*. 2010;10 (4 Pt 2):1069-1080.
21. *U.S. Renal Data System, USRDS 2014 Annual Data Report: Atlas of End-Stage Renal Disease in the United States.*; 2014. <http://www.usrds.org/Default.aspx>.
22. Canadian Institute for Health Information. *Deceased Organ Donor Potential in Canada*. Ottawa, ON; 2014.
23. Metzger R, Delmonico FL, Feng S, Port FK, Wynn JJ, Merion RM. Expanded criteria donors for kidney transplantation. *Am J Transplant*. 2003;3 Suppl 4:114-125.
24. Summers DM, Watson CJE, Pettigrew GJ, et al. Kidney donation after circulatory death (DCD): state of the art. *Kidney Int*. 2015;(Dcd):1-9. doi:10.1038/ki.2015.88.
25. Campbell GMD, Sutherland FR. Non-heart-beating organ donors as a source of kidneys for transplantation: A chart review. *Cmaj*. 1999;160(11):1573-1576.
26. Gagandeep S, Matsuoka L, Mateo R, et al. Expanding the donor kidney pool: utility of renal allografts procured in a setting of uncontrolled cardiac death. *Am J Transplant*. 2006;6(7):1682-1688. doi:10.1111/j.1600-6143.2006.01386.x.
27. O'Neill S, Gallagher K, Hughes J, Wigmore SJ, Ross J a, Harrison EM. Challenges in early clinical drug development for ischemia-reperfusion injury in kidney transplantation. *Expert Opin Drug Discov*. 2015;10(7):753-762. doi:10.1517/17460441.2015.1044967.
28. Oniscu GC, Randle L V., Muiesan P, et al. In Situ Normothermic Regional Perfusion for Controlled Donation After Circulatory Death-The United Kingdom Experience. *Am J Transplant*. 2014;14(12):2846-2854. doi:10.1111/ajt.12927.

29. Summers DM, Johnson RJ, Hudson A, Collett D, Watson CJ, Bradley JA. Effect of donor age and cold storage time on outcome in recipients of kidneys donated after circulatory death in the UK: A cohort study. *Lancet*. 2013;381(9868):727-734. doi:10.1016/S0140-6736(12)61685-7.
30. Cho YW, Terasaki PI, Cecka JM GD. Transplantation of kidneys from donors whose hearts have stopped beating. *N Engl J Med*. 1998;338:221-225.
31. Akoh J. Kidney donation after cardiac death. *World J Nephrol*. 2012;1(3):79. doi:10.5527/wjn.v1.i3.79.
32. Galliford J, Game DS. Modern renal transplantation: present challenges and future prospects. *Postgrad Med J*. 2009;85(1000):91-101. doi:10.1136/pgmj.2008.070862.
33. Chandran S, Vincenti F. Clinical Aspects: Focusing on Key Unique Organ-Specific Issues of Renal Transplantation. *Cold Spring Harb Perspect Med*. 2014;4(2):a015644-a015644. doi:10.1101/cshperspect.a015644.
34. McDonald SP. Survival of recipients of cadaveric kidney transplants compared with those receiving dialysis treatment in Australia and New Zealand, 1991-2001. *Nephrol Dial Transplant*. 2002;17(12):2212-2219. doi:10.1093/ndt/17.12.2212.
35. Tonelli M, Wiebe N, Knoll G, et al. Systematic review: Kidney transplantation compared with dialysis in clinically relevant outcomes. *Am J Transplant*. 2011;11(10):2093-2109. doi:10.1111/j.1600-6143.2011.03686.x.
36. Greco F, Fornara P, Mirone V. Renal transplantation: Technical aspects, diagnosis and management of early and late urological complications. *Panminerva Med*. 2014;56(1):17-29.
37. Jassal S V, Krahn MD, Naglie G, et al. Kidney transplantation in the elderly: a decision analysis. *J Am Soc Nephrol*. 2003;14(1):187-196. doi:10.1097/01.ASN.0000042166.70351.57.

38. Schnuelle P, Lorenz D, Trede M, Van Der Woude F. Impact of renal cadaveric transplantation on survival in end-stage renal failure: Evidence for reduced mortality risk compared with hemodialysis during long-term follow-up. *J Am Soc Nephrol*. 1998;9:2135-2141.
39. Wolfe RA, Ashby VB, Milford EL, et al. Comparison of mortality in all patients on dialysis, patients on dialysis awaiting transplantation, and recipients of a first cadaveric transplant. *N Engl J Med*. 1999;341(23):1725-1730. doi:10.1056/NEJM199912023412303.
40. Rao P, Merion R, Ashby V, Port F, Wolfe R, Kayler L. Renal transplantation in elderly patients older than 70 years of age: results from the Scientific Registry of Transplant Recipients. *Transplantation*. 2007;83(8):1069-1074.
41. Meier-Kriesche H-U, Schold JD, Srinivas TR, Reed A, Kaplan B. Kidney transplantation halts cardiovascular disease progression in patients with end-stage renal disease. *Am J Transplant*. 2004;4(10):1662-1668. doi:10.1111/j.1600-6143.2004.00573.x.
42. Perović S, Janković S. Renal transplantation vs hemodialysis: Cost-effectiveness analysis. *Vojnosanit Pregl*. 2009;66(8):639-644. doi:10.2298/VSP0908639P.
43. Eltzschig HK, Eckle T. Ischemia and reperfusion—from mechanism to translation. *Nat Med*. 2011;17(11):1391-1401. doi:10.1038/nm.2507.
44. Duehrkop C, Rieben R. Ischemia/reperfusion injury: Effect of simultaneous inhibition of plasma cascade systems versus specific complement inhibition. *Biochem Pharmacol*. 2014;88(1):12-22. doi:10.1016/j.bcp.2013.12.013.
45. Marsden VS, Strasser A. Control of apoptosis in the immune system: Bcl-2, BH3-only proteins and more. *Annu Rev Immunol*. 2003;21(1):71-105. doi:10.1146/annurev.immunol.21.120601.141029.
46. Adams JM, Cory S. Bcl-2-regulated apoptosis: mechanism and therapeutic potential. *Curr Opin Immunol*. 2007;19(5):488-496. doi:10.1016/j.coi.2007.05.004.



47. Hotchkiss RS, Strasser A, McDunn JE, Swanson PE. Cell death. *N Engl J Med*. 2009;361(16):1570-1583. doi:10.1056/NEJMra0901217.
48. Klionsky DJ. Autophagy: from phenomenology to molecular understanding in less than a decade. *Nat Rev Mol Cell Biol*. 2007;8(11):931-937. doi:10.1038/nrm2245.
49. Kroemer G, Jäätelä M. Lysosomes and autophagy in cell death control. *Nat Rev Cancer*. 2005;5(11):886-897. doi:10.1038/nrc1738.
50. Guan L-Y, Fu P-Y, Li P-D, et al. Mechanisms of hepatic ischemia-reperfusion injury and protective effects of nitric oxide. *World J Gastrointest Surg*. 2014;6(7):122-128. doi:10.4240/wjgs.v6.i7.122.
51. Malek M, Nematbakhsh M. Renal ischemia / reperfusion injury ; from pathophysiology to treatment. *J Ren Inj Prev*. 2015;4(2):20-27. doi:10.12861/jrip.2015.06.
52. Sastre J, Serviddio G, Pereda J, et al. Mitochondrial function in liver disease. *Front Biosci*. 2007;12:1200-1209.
53. Aguilar HI, Botla R, Arora AS, Bronk SF, Gores GJ. Induction of the mitochondrial permeability transition by protease activity in rats: A mechanism of hepatocyte necrosis. *Gastroenterology*. 1996;110(2):558-566. doi:10.1053/gast.1996.v110.pm8566604.
54. Crow MT. The Mitochondrial Death Pathway and Cardiac Myocyte Apoptosis. *Circ Res*. 2004;95(10):957-970. doi:10.1161/01.RES.0000148632.35500.d9.
55. Kluck RM, Bossy-Wetzell E, Green DR, Newmeyer DD. The release of cytochrome c from mitochondria: a primary site for Bcl-2 regulation of apoptosis. *Science*. 1997;275(5303):1132-1136. doi:10.1126/science.275.5303.1132.
56. Du C, Fang M, Li Y, Li L, Wang X. Smac, a mitochondrial protein that promotes cytochrome c-dependent caspase activation by eliminating IAP inhibition. *Cell*. 2000;102(1):33-42. doi:10.1016/S0092-8674(00)00008-8.

57. Stratford May JW, Deng X. *Principles of Molecular Medicine*. Vol 2nd ed. (Runge MS, Patterson C, eds.). Totowa, NJ: Humana Press; 2006. doi:10.1007/978-1-59259-963-9.
58. Wang R. Two's company, three's a crowd: can H<sub>2</sub>S be the third endogenous gaseous transmitter? *FASEB J*. 2002;16(13):1792-1798. doi:10.1096/fj.02-0211hyp.
59. Bogdan C. Nitric oxide and the immune response. *Nat Immunol*. 2001;2(10):907-916. doi:10.1038/ni1001-907.
60. Snijder PM, Van Den Berg E, Whiteman M, Bakker SJL, Leuvenink HGD, Van Goor H. Emerging role of gasotransmitters in renal transplantation. *Am J Transplant*. 2013;13(12):3067-3075. doi:10.1111/ajt.12483.
61. Maines MD, Gibbs PEM. 30 Some years of heme oxygenase: From a "molecular wrecking ball" to a "mesmerizing" trigger of cellular events. *Biochem Biophys Res Commun*. 2005;338(1):568-577. doi:10.1016/j.bbrc.2005.08.121.
62. Otterbein LE, Bach FH, Alam J, et al. Carbon monoxide has anti-inflammatory effects involving the mitogen-activated protein kinase pathway. *Nat Med*. 2000;6(4):422-428. doi:10.1038/74680.
63. Otterbein LE, Zuckerbraun BS, Haga M, et al. Carbon monoxide suppresses arteriosclerotic lesions associated with chronic graft rejection and with balloon injury. *Nat Med*. 2003;9(2):183-190. doi:10.1038/nm817.
64. Chin BY, Jiang G, Wegiel B, et al. Hypoxia-inducible factor 1alpha stabilization by carbon monoxide results in cytoprotective preconditioning. *Proc Natl Acad Sci U S A*. 2007;104(12):5109-5114. doi:10.1073/pnas.0609611104.
65. Warenycia MW, Goodwin LR, Benishin CG, Reiffenstein, R. J. Francom DM, Taylor JD, Dieken FP. Acute hydrogen sulfide poisoning: demonstration of selective uptake of sulfide by the brainstem by measurement of brain sulfide levels. *Biochem Pharmacol*. 1989;38:973-981.

66. Abe K, Kimura H. The possible role of hydrogen sulfide as an endogenous neuromodulator. *Off J Soc Neurosci*. 1996;16(3):1066-1071.
67. Zhong G, Chen F, Cheng Y, Tang C, Du J. The role of hydrogen sulfide generation in the pathogenesis of hypertension in rats induced by inhibition of nitric oxide synthase. *Journal of hypertension. J Hypertens*. 2003;21:1879-1885.
68. Zhao W, Zhang J, Lu Y, Wang R. The vasorelaxant effect of H<sub>2</sub>S as a novel endogenous gaseous KATP channel opener. *EMBO J*. 2001;20:6008-6016.
69. Dombkowski RA, Russell MJ, Olson KR. Hydrogen sulfide as an endogenous regulator of vascular smooth muscle tone in trout. *Am J Physiol Regul Integr Comp Physiol*. 2004;286(4):R678-R685. doi:10.1152/ajpregu.00419.2003.
70. Hosoki R, Matsuki N, Kimura H. The possible role of hydrogen sulfide as an endogenous smooth muscle relaxant in synergy with nitric oxide. *Biochem Biophys Res Commun*. 1997;237(3):527-531. doi:10.1006/bbrc.1997.6878.
71. Kolluru GK, Shen X, Bir SC, Kevil CG. Hydrogen sulfide chemical biology: pathophysiological roles and detection. *Nitric Oxide*. 2013;35:5-20. doi:10.1016/j.niox.2013.07.002.
72. Zanardo RCO, Brancalone V, Distrutti E, Fiorucci S, Cirino G, Wallace JL. Hydrogen sulfide is an endogenous modulator of leukocyte-mediated inflammation. *FASEB J*. 2006;20(12):2118-2120. doi:10.1096/fj.06-6270fje.
73. Yonezawa D, Sekiguchi F, Miyamoto M, et al. A protective role of hydrogen sulfide against oxidative stress in rat gastric mucosal epithelium. *Toxicology*. 2007;241(1-2):11-18. doi:10.1016/j.tox.2007.07.020.
74. Laggner H, Hermann M, Esterbauer H, et al. The novel gaseous vasorelaxant hydrogen sulfide inhibits angiotensin-converting enzyme activity of endothelial cells. *J Hypertens*. 2007;25(10):2100-2104. doi:10.1097/HJH.0b013e32829b8fd0.

75. Ali MY, Whiteman M, Low CM, Moore PK. Hydrogen sulphide reduces insulin secretion from HIT-T15 cells by a KATP channel-dependent pathway. *J Endocrinol.* 2007;195(1):105-112. doi:10.1677/JOE-07-0184.
76. Yang G, Zhao K, Ju Y, et al. Hydrogen Sulfide Protects Against Cellular Senescence via S-Sulphydration of Keap1 and Activation of Nrf2. *Antioxid Redox Signal.* 2013;18(15):1906-1919. doi:10.1089/ars.2012.4645.
77. Calvert JW, Jha S, Gundewar S, et al. Hydrogen sulfide mediates cardioprotection through nrf2 signaling. *Circ Res.* 2009;105(4):365-374. doi:10.1161/CIRCRESAHA.109.199919.
78. Chung KF. Hydrogen sulfide as a potential biomarker of asthma. *Expert Rev Respir Med.* 2014;8(1):5-13. doi:10.1586/17476348.2014.856267.
79. Chen YH, Yao WZ, Geng B, et al. Endogenous hydrogen sulfide in patients with COPD. *Chest.* 2005;128(5):3205-3211. doi:10.1378/chest.128.5.3205.
80. Fu Z, Liu X, Geng B, Fang L, Tang C. Hydrogen sulfide protects rat lung from ischemia–reperfusion injury. *Life Sci.* 2008;82(23-24):1196-1202. doi:10.1016/j.lfs.2008.04.005.
81. Jha S, Calvert JW, Duranski MR, Ramachandran A, Lefer DJ. Hydrogen sulfide attenuates hepatic ischemia-reperfusion injury: role of antioxidant and antiapoptotic signaling. *AJP Hear Circ Physiol.* 2008;295(2):H801-H806. doi:10.1152/ajpheart.00377.2008.
82. Sodha NR, Clements RT, Feng J, et al. The effects of therapeutic sulfide on myocardial apoptosis in response to ischemia–reperfusion injury☆☆☆. *Eur J Cardio-Thoracic Surg.* 2008;33(5):906-913. doi:10.1016/j.ejcts.2008.01.047.
83. Elrod JW, Calvert JW, Morrison J, et al. Hydrogen sulfide attenuates myocardial ischemia-reperfusion injury by preservation of mitochondrial function. *Proc Natl Acad Sci.* 2007;104(39):15560-15565. doi:10.1073/pnas.0705891104.

84. Bos EM, Leuvenink HGD, Snijder PM, et al. Hydrogen sulfide-induced hypometabolism prevents renal ischemia/reperfusion injury. *J Am Soc Nephrol.* 2009;20(9):1901-1905. doi:10.1681/ASN.2008121269.
85. Koning AM, Frenay A-RS, Leuvenink HGD, van Goor H. Hydrogen sulfide in renal physiology, disease and transplantation – The smell of renal protection. *Nitric Oxide.* 2015;46:37-49. doi:10.1016/j.niox.2015.01.005.
86. Winyard PG, Blake DR, Evans CH, eds. *Free Radicals and Inflammation.* Basel: Birkhäuser Basel; 2000. doi:10.1007/978-3-0348-8482-2.
87. Whiteman M, Winyard PG. Hydrogen sulfide and inflammation: the good, the bad, the ugly and the promising. *Expert Rev Clin Pharmacol.* 2011;4(1):13-32. doi:10.1586/ecp.10.134.
88. Cheung NS, Peng ZF, Chen MJ, Moore PK, Whiteman M. Hydrogen sulfide induced neuronal death occurs via glutamate receptor and is associated with calpain activation and lysosomal rupture in mouse primary cortical neurons. *Neuropharmacology.* 2007;53(4):505-514. doi:10.1016/j.neuropharm.2007.06.014.
89. Sodha NR, Clements RT, Feng J, et al. The effects of therapeutic sulfide on myocardial apoptosis in response to ischemia-reperfusion injury. *Eur J Cardio-thoracic Surg.* 2008;33(5):906-913. doi:10.1016/j.ejcts.2008.01.047.
90. Zhu JXG, Kalbfleisch M, Yang YX, et al. Detrimental effects of prolonged warm renal ischaemia-reperfusion injury are abrogated by supplemental hydrogen sulphide: An analysis using real-time intravital microscopy and polymerase chain reaction. *BJU Int.* 2012;110(11 C). doi:10.1111/j.1464-410X.2012.11555.x.
91. Baud V, Karin M. Signal transduction by tumor necrosis factor and its relatives. *Trends Cell Biol.* 2001;9:372-377.
92. Bradley J. TNF-mediated inflammatory disease. *J Pathol.* 2008;2:149-160.

93. Yoshida L, Tsunawaki S. Expression of NADPH oxidases and enhanced H<sub>2</sub>O<sub>2</sub>-generating activity in human coronary artery endothelial cells upon induction with tumor necrosis factor- $\alpha$ . *Int Immunopharmacol*. 2008;10:1377-1385.
94. Zelová H, Hošek J. TNF- $\alpha$  signalling and inflammation: interactions between old acquaintances. *Inflamm Res*. 2013;62(7):641-651. doi:10.1007/s00011-013-0633-0.
95. McCord JM, Fridovich I. The reduction of cytochrome c by milk xanthine oxidase. *J Biol Chem*. 1968;243(21):5753-5760. doi:4972775.
96. Nakano H, Nakajima A, Sakon-Komazawa S, Piao J-H, Xue X, Okumura K. Reactive oxygen species mediate crosstalk between NF- $\kappa$ B and JNK. *Cell Death Differ*. 2006;13(5):730-737. doi:10.1038/sj.cdd.4401830.
97. Whiteman M, Li L, Kostetski I, et al. Evidence for the formation of a novel nitrosothiol from the gaseous mediators nitric oxide and hydrogen sulphide. *Biochem Biophys Res Commun*. 2006;343(1):303-310. doi:10.1016/j.bbrc.2006.02.154.
98. Schreier SM, Muellner MK, Steinkellner H, et al. Hydrogen Sulfide Scavenges the Cytotoxic Lipid Oxidation Product 4-HNE. *Neurotox Res*. 2010;17(3):249-256. doi:10.1007/s12640-009-9099-9.
99. Whiteman M, Armstrong JS, Chu SH, et al. The novel neuromodulator hydrogen sulfide: an endogenous peroxynitrite “scavenger”? *J Neurochem*. 2004;90(3):765-768. doi:10.1111/j.1471-4159.2004.02617.x.
100. Whiteman M, Cheung NS, Zhu Y-Z, et al. Hydrogen sulphide: a novel inhibitor of hypochlorous acid-mediated oxidative damage in the brain? *Biochem Biophys Res Commun*. 2005;326(4):794-798. doi:10.1016/j.bbrc.2004.11.110.
101. Geng B, Chang L, Pan C, et al. Endogenous hydrogen sulfide regulation of myocardial injury induced by isoproterenol. *Biochem Biophys Res Commun*. 2004;318(3):756-763. doi:10.1016/j.bbrc.2004.04.094.

102. Fu M, Zhang W, Wu L, Yang G, Li H, Wang R. Hydrogen sulfide (H<sub>2</sub>S) metabolism in mitochondria and its regulatory role in energy production. *Proc Natl Acad Sci*. 2012;109(8):2943-2948. doi:10.1073/pnas.1115634109.
103. Guo W, Kan J, Cheng Z, et al. Hydrogen Sulfide as an Endogenous Modulator in Mitochondria and Mitochondria Dysfunction. *Oxid Med Cell Longev*. 2012;2012:1-9. doi:10.1155/2012/878052.
104. Sivarajah A, Collino M, Yasin M, et al. Anti-apoptotic and anti-inflammatory effects of hydrogen sulfide in a rat model of regional myocardial I/R. *Shock*. 2009;31(3):267-274. doi:10.1097/SHK.0b013e318180ff89.
105. Shibuya N, Kimura H. Production of hydrogen sulfide from D-cysteine and its therapeutic potential. *Front Endocrinol (Lausanne)*. 2013;4(JUL):1-5. doi:10.3389/fendo.2013.00087.
106. Shibuya N, Koike S, Tanaka M, et al. A novel pathway for the production of hydrogen sulfide from D-cysteine in mammalian cells. *Nat Commun*. 2013;4:1366. doi:10.1038/ncomms2371.
107. Whiteman M, Le Trionnaire S, Chopra M, Fox B, Whatmore J. Emerging role of hydrogen sulfide in health and disease: critical appraisal of biomarkers and pharmacological tools. *Clin Sci (Lond)*. 2011;121(11):459-488. doi:10.1042/CS20110267.
108. Li L, Whiteman M, Guan YY, et al. Characterization of a novel, water-soluble hydrogen sulfide-releasing molecule (GYY4137): New insights into the biology of hydrogen sulfide. *Circulation*. 2008;117(18):2351-2360. doi:10.1161/CIRCULATIONAHA.107.753467.
109. Whiteman M, Perry A, Zhou Z, et al. Chemistry, Biochemistry and Pharmacology of Hydrogen Sulfide. 2015;230. doi:10.1007/978-3-319-18144-8.
110. Fox B, Schantz JT, Haigh R, et al. Inducible hydrogen sulfide synthesis in chondrocytes and mesenchymal progenitor cells: Is H<sub>2</sub>S a novel cytoprotective

- mediator in the inflamed joint? *J Cell Mol Med.* 2012;16(4):896-910.  
doi:10.1111/j.1582-4934.2011.01357.x.
111. Hine C, Harputlugil E, Zhang Y, et al. Endogenous Hydrogen Sulfide Production Is Essential for Dietary Restriction Benefits. *Cell.* 2015;160(1-2):132-144.  
doi:10.1016/j.cell.2014.11.048.
112. Lobb I, Mok A, Lan Z, Liu W, Garcia B, Sener A. Supplemental hydrogen sulphide protects transplant kidney function and prolongs recipient survival after prolonged cold ischaemia-reperfusion injury by mitigating renal graft apoptosis and inflammation. *BJU Int.* 2012;110(11 C). doi:10.1111/j.1464-410X.2012.11526.x.
113. Bos EM, Wang R, Snijder PM, et al. Cystathionine  $\gamma$ -Lyase Protects against Renal Ischemia/Reperfusion by Modulating Oxidative Stress. *J Am Soc Nephrol.* 2013;24(5):759-770. doi:10.1681/ASN.2012030268.
114. Ueda N, Kaushal GP, Hong X, Shah S V. Role of enhanced ceramide generation in DNA damage and cell death in chemical hypoxic injury to LLC-PK1 cells. *Kidney Int.* 1998;54(2):399-406. doi:10.1046/j.1523-1755.1998.00008.x.
115. Kurian GA, Pemaih B. Standardization of in vitro Cell-based Model for Renal Ischemia and Reperfusion Injury. *Indian J Pharm Sci.* 2014;76(4):348-353.  
doi:10.1016/S0140-6736(68)90219-5.
116. Hotter G, Palacios L, Sola A. Low O<sub>2</sub> and high CO<sub>2</sub> in LLC-PK1 cells culture mimics renal ischemia-induced apoptosis. *Lab Invest.* 2004;84(2):213-220.  
doi:10.1038/labinvest.3700026.
117. Wiegele G, Brandis M, Zimmerhackl LB. Apoptosis and necrosis during ischaemia in renal tubular cells (LLC-PK1 and MDCK). *Nephrol Dial Transplant.* 1998;13(5):1158-1167. doi:10.1093/ndt/13.5.1158.
118. Yang C, Yang Z, Zhang M, et al. Hydrogen sulfide protects against chemical hypoxia-induced cytotoxicity and inflammation in hacat cells through inhibition of



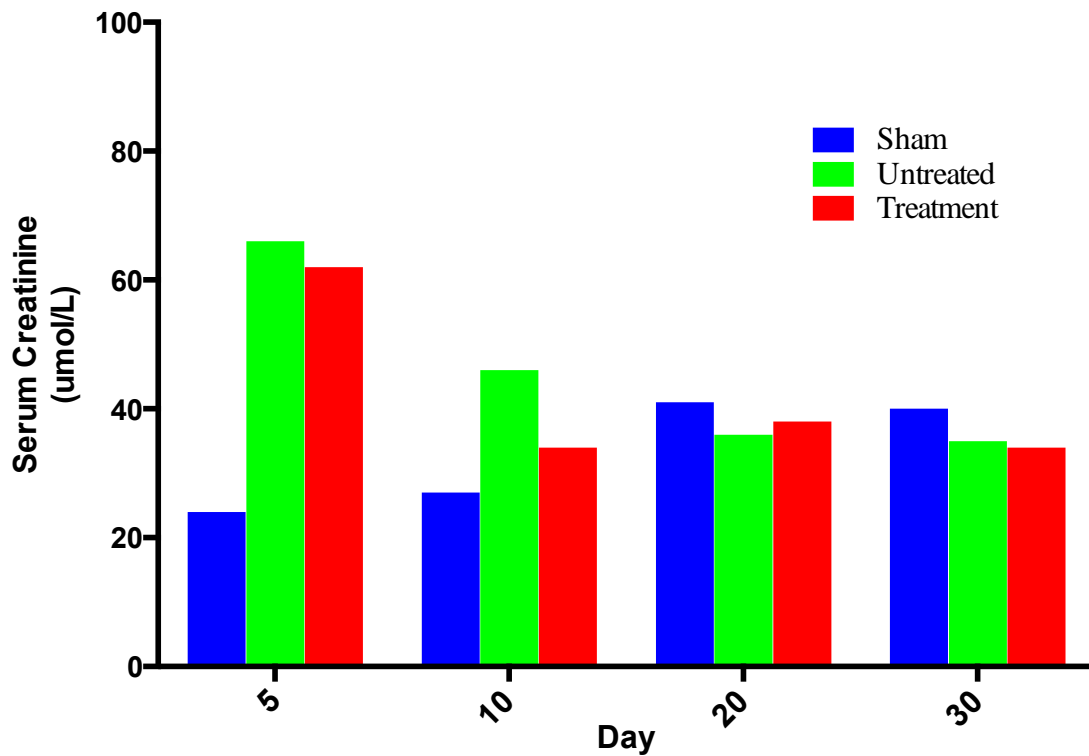
- ROS/NF-kB/COX-2 pathway. *PLoS One*. 2011;6(7).  
doi:10.1371/journal.pone.0021971.
119. Henderson PW, Singh SP, Belkin D, et al. Hydrogen Sulfide Protects Against Ischemia-Reperfusion Injury in an In Vitro Model of Cutaneous Tissue Transplantation. *J Surg Res*. 2010;159(1):451-455. doi:10.1016/j.jss.2009.05.010.
120. Bursch W, Kleine L, Tenniswood M. The biochemistry of cell death by apoptosis. *Biochem Cell Biol*. 1990;88:1071-1074.
121. Bursch W, Paffe S, Putz B, Barthel G, Schulte- Hermann R. Determination of the length of the Apoptosis Assays 389 histological stages of apoptosis in normal liver and in altered hepatic foci in rats. *Carcinogenesis*. 1990;11:847-853.
122. Walrand S, Valeix S, Rodriguez C, Ligot P, Chassagne J, Vasson MP. Flow cytometry study of polymorphonuclear neutrophil oxidative burst: A comparison of three fluorescent probes. *Clin Chim Acta*. 2003;331(1-2):103-110.  
doi:10.1016/S0009-8981(03)00086-X.
123. Turrens JF, Boveris A. Generation of superoxide anion by the NADH dehydrogenase of bovine heart mitochondria. *Biochem J*. 1980;191(2):421-427.
124. Turrens JF, Freeman BA, Levitt JG, Crapo JD. The effect of hyperoxia on superoxide production by lung submitochondrial particles. *Arch Biochem Biophys*. 1982;217(2):401-410. doi:10.1016/0003-9861(82)90518-5.
125. Green DR, Kroemer G. The pathophysiology of mitochondrial cell death. *Science*. 2004;305(5684):626-629. doi:10.1126/science.1099320.
126. Knudson CM, Brown NM. Mitochondria potential, bax “activation,” and programmed cell death. *Methods Mol Biol*. 2008;414:95-108.
127. Pirot AL, Fritz KI, Ashraf QM, Mishra OP, Delivoria-Papadopoulos M. Effects of severe hypocapnia on expression of Bax and Bcl-2 proteins, DNA fragmentation,

and membrane peroxidation products in cerebral cortical mitochondria of newborn piglets. *Neonatology*. 2007;91(1):20-27. doi:10.1159/000096967.

128. Kroemer G, Galluzzi L, Brenner C. Mitochondrial Membrane Permeabilization in Cell Death. *Physiol Rev*. 2007;87(1):99-163. doi:10.1152/physrev.00013.2006.
129. De Marchi U, Campello S, Szabò I, Tombola F, Martinou JC, Zoratti M. Bax does not directly participate in the Ca<sup>2+</sup>-induced permeability transition of isolated mitochondria. *J Biol Chem*. 2004;279(36):37415-37422. doi:10.1074/jbc.M314093200.

## Appendices

### Appendix A: Preliminary data showing graft recovery following renal transplantation with grafts that had experienced IRI.



Serum creatinine levels of renal transplant recipients after receiving donor kidneys that were clamped for 20 minutes and underwent a cold ischemic period of 18 hours in UW solution only (untreated group), D-cysteine pre-op and UW solution plus 150 $\mu$ M NaHS (treatment group) as well as sham-operated rats. (Mean values are shown, n=1)

## Appendix B: Ethics approval form for *in-vivo* experiments



AUP Number: 2013-049  
PI Name: Sener, Alp  
AUP Title: Renal Ischemia-Reperfusion Injury/Rats

**Official Notification of AUS Approval:** A MODIFICATION to Animal Use Protocol 2013-049 has been approved.

The holder of this Animal Use Protocol is responsible to ensure that all associated safety components (biosafety, radiation safety, general laboratory safety) comply with institutional safety standards and have received all necessary approvals. Please consult directly with your institutional safety officers.

Submitted by: Kinchlea, Will D  
on behalf of the Animal Use Subcommittee

*The University of Western Ontario*  
Animal Use Subcommittee / University Council on Animal Care  
Health Sciences Centre, • London, Ontario • CANADA – N6A 5C1  
PH: 519-661-2111 ext. 86768 • FL 519-661-2028  
Email: [auspc@uwo.ca](mailto:auspc@uwo.ca) • <http://www.uwo.ca/animal/website/>

## Curriculum Vitae

**Name:** Jaskirandeep Kaur Grewal

**Post-secondary  
Education and  
Degrees:** University of Windsor  
Windsor, Ontario, Canada  
2009-2013 B.Sc. Honors

The University of Western Ontario  
London, Ontario, Canada  
2013-2015 M.Sc.

**Honors and  
Awards:** Western Graduate Research Scholarship (WGRS)  
2013-2015

Microbiology and Immunology Travel Award  
2015

**Related Work  
Experience** Teaching Assistant  
The University of Western Ontario  
2013-2015

Tutor, Indigenous Services  
The University of Western Ontario  
2014-2015

**Conference:**  
Oral Presentation at American Transplant Congress 2015, Philadelphia, PA, USA.

**Published Abstract:**

Hydrogen Sulfide Restores Protective Capacity of University of Wisconsin Solution  
During Normothermic Preservation  
*J. Grewal, I. Lobb, M. Whiteman and A. Sener; American Journal of Transplantation  
2015; 15 (suppl 3)*